Journal of
Civil Engineering and Architecture

Volume 13, Number 3, March 2019

Journal of Civil Engineering and Architecture

David Publishing Company
www.davidpublisher.com

Journal of Civil Engineering and Architecture

Contents

Mosul Dam: Geology and Safety Concerns

Nasrat Adamo[1], Nadhir Al-Ansari[2], Varoujan Sissakian[3], Jan Laue[2] and Sven Knutsson[2]

1. Private Consultant Engineering, Sågaregränd 3 lgh 100260358 Norrköping, Sweden

2. Lulea University of Technology, Lulea 97187, Sweden

3. University of Kurdistan, Howler, KRG, Iraq and Private Consultant Geologist, Erbil 44001, Iraq

Abstract: Mosul Dam is an earth fill dam located on the River Tigris northern part of Iraq. The capacity of its reservoir is 11.11 billion cubic meters which makes it the fourth biggest dam in the Middle East. From geological perspective, the dam is located on double plunging anticlines. The rocks of the site are mainly composed of highly jointed and karistified alternating beds of limestones, gysum and marls, since the impoundment of the reservoir seepage of water was recognized under the foundation of the dam. To stop or minimize the seepage, intensive grouting operations were conducted. Recent investigations and evaluation of the conditions of the dam indicate that it is in a critical situation. In this paper, consequences of the dam failure are discussed and possible solutions are given.

Key words: Mosul Dam, karst, infiltration, dam foundation, dam failure.

1. Introduction

Mosul Dam, the largest dam in Iraq, is also one of the large dams in the world and the fourth largest reservoir in the Middle East. It is located on the Tigris river in northern Iraq approximately 50 kilometers north west of Mosul city and 80 kilometers from the Syrian and Turkish borders.

Although the dam is about 500 km on a straight line distance to the north from Baghdad a flood wave study showed that such wave resulting from the dam collapse could reach Baghdad within 48 hours causing devastating results for the whole reach and its population.

The maps in Figs. 1 and 2 show the location of this dam.

2. History

Mosul dam site was first investigated in 1952 by an American firm, after which four investigation campaigns were conducted in the sixties and seventies. The first three reports prepared by American, Finish and Soviet consultants agreed on the difficulties

involved in the site for the construction of a high dam based on the conditions of foundations due to the presence of gypsum, gypsum anhydride and gypsum breccias. The fourth study report prepared by Swiss consultants concluded that the dam can be built and that the foundation can be sealed by intensive blanket grouting together with a deep grout curtain. A conclusion which proved later on to be very short sighted. The construction of the dam was initiated in 1980 and completed in 1985. The first sign of trouble appeared at the first filling in the spring of 1986 [1]. Maintenance foundation treatment by continuous massive grouting program was envisaged as a solution, but the problem persisted and mass grouting continued ever since as a maintenance measure with no signs of an end in the future. Moreover sinkholes which had started to form since the filling of reservoir evolved into common phenomena [2, 3].

3. Dams Features

Mosul Dam scheme consists of three parts:

(1) Mosul 1, which is the main embankment dam and main power station.

(2) Mosul 2, the re-regulating dam and power station located 9.1 km downstream of the main dam; distance

---

Corresponding author: Nadhir A. Al-Ansari, professor, research fields: water resources and environment.

Fig. 1   Mosul Dam location Ma.

Fig. 2   Map of Iraq indicating Mosul Dam site.

measured along river course.

(3) Mosul 3, the pump storage scheme (200 Mw).

We are focused here on the Main Dam as it is the source of troubles encountered in this Scheme; in the following Fig. 3 both upstream and downstream views are shown. The dam's layout and appurtenant structures arrangement are shown in Fig. 4.

Mosul Dam is an earth fill dam with concrete spillway with a maximum discharge capacity of 12,000 m^3/second and powerhouse. Two low level bottom outlets are provided for emptying the reservoir in case

of an emergency. The maximum height of the dam is 113 meters while total length is 3,400 meters, and the total volume of fill is about 38 million cubic meters. The embankment has a clay core in the middle and gravel shells on the exterior slopes and provided with two layers of filters on each side of the core. An emergency concrete/earthfill fuse plug 400 meters long is incorporated in the embankment to safeguard against overtopping. The maximum discharge of this facility is 4,000 cubic meters per second at the maximum water level. The service spillway is a conventional ogee weir

Fig. 3 Mosul Dam: upstream view (left), downstream view (right).
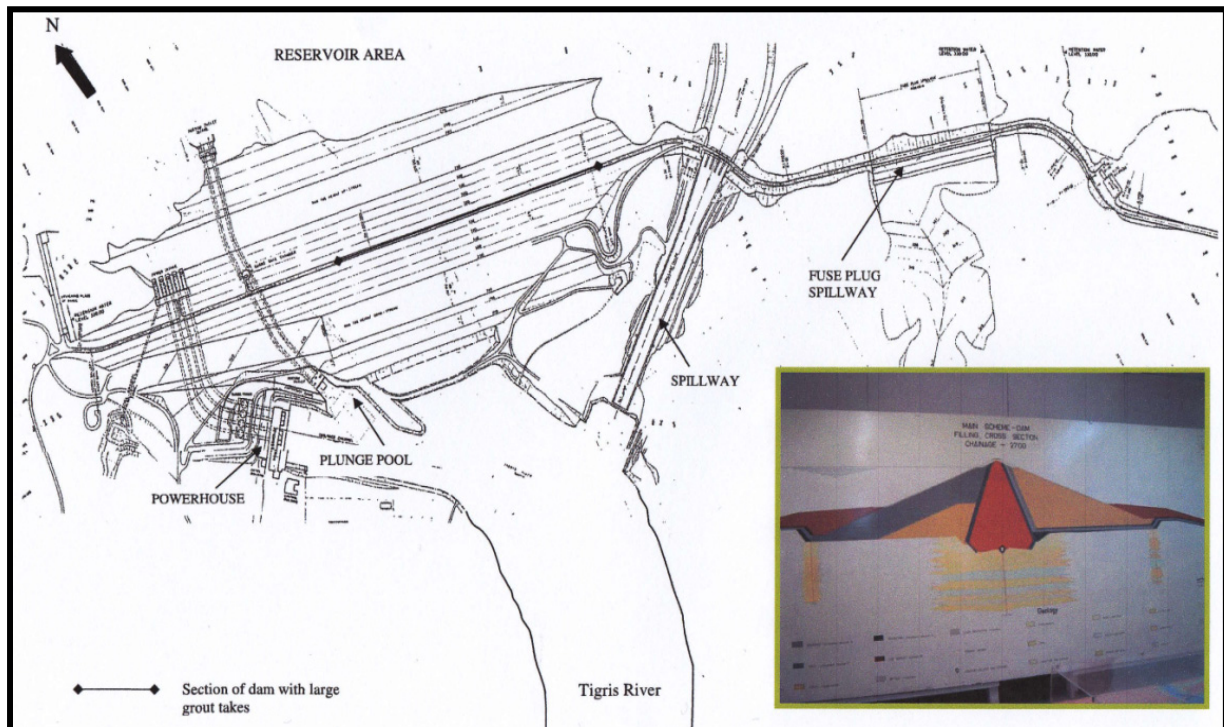
Fig. 4 Mosul Dam general arrangement.

type headwork, rectangular chute and flip bucket structure with discharge capacity of 12,400 cubic meters per second at the maximum flood water level 335 masl and 8,000 cubic meter per second at the maximum operation water level (330 masl).

The dam serves the functions of flood protection, providing irrigation water and power generation. The main power station has an installed capacity of 750 Mw and a 50 Mw PowerStation was planned for the Jazira main canal off take (not constructed yet). Additionally a 60 Mw installed capacity is provided at a re-regulation facility downstream of the main dam, and a pump storage station of 200 Mw installed capacity is constructed on the right hand high bank making total installed capacity more than 1,050 Mw [4].

Main operational features of the dam are as shown in Table 1:

Table 1   Main operational features of Mosul Dam [4].

Description	Unit	Value	Remarks
Dam Height	m	113	
Total Storage at El.330m.a.s.l	Km^3	11.11	
Live Storage (Usable for Irrigation and Power Generation)	Km^3	8.16	
Dead Storage at El.300m.a.s.l	Km^3	2.95	Power Station stops operation
Available Capacity for flood Routing (From El. 330m.a.s l to El.335m.a.sl)	Km^3	2.03	To Route 1:10000 years flood
Irrigated Area (Directly from Mosul Reservoir)	ha	250000	North Jazira,East Jazira and South Jazira Projects
Irrigated Area from dams releases at the middle and south of Iraq	ha	750000	
Total Installed Capacity in the three power stations of the Project	MW	1050	Main dam PS..Reregulating dam PS.& Pump storage Scheme PS.
Total Annual Power Generation	GWH	3400	

4. Regional Geology

The geology of the dam area belongs to the Pleistocene to recent age alluvial deposits overlaying rocks of the Lower to Middle Miocene age Lower Fars Group (Fatha Formation) which is formed of highly karstified layers of limestone and soluble gypsum, followed by Oligocene to Lower Miocene age Jeribe limestone formation. The geomorphology of Mosul dam area is characterized by hilly terrain that rises to low mountainous area. The mountain anticlines trend NW-SE direction and change to almost E-W direction. Fig. 5 is a Google image of the dam and surrounding area.

Another significant morphological aspect in the area is karstification in the area and in the dam site [5, 6]. Typical dissolution karstification phenomena close to the dam site and sinkholes are shown in Figs. 6-9. While sinkholes have developed very close to the dam during and after operation, and similarly sinkholes were discovered in the reservoir later on as shown in Fig. 10 [7].

5. Geological Conditions at the Dam Site

The main geological factors influencing the dam safety are given below and their effects will be discussed later on. These factors are:

(1) The karsts prevailing in the dam site and in the reservoir area.

(2) The existence of gypsum/anhydrite rock formations in dam foundation alternating with soft marl layers and weathered and cavernous limestone beddings.

(3) The presence of extensive ground water aquifer called Der Wadi Maleh aquifer in the dam site.

Figs. 9 and 10 shown already indicate the extent of the karsts phenomena in the form of sinkholes upstream area of the dam and in the reservoir.

The continual development of such sinkholes will open new connections with the groundwater aquifer running below and around the dam site causing more dissolution problems.

The existence of highly karstified and jointed limestone layers in the dam foundations gave rise to the

Fig. 5   Google Earth image of the Mosul Dam site, located within Butma east Anticline. AR = anticlinal ridge, FI = flat iron [5].

Fig. 6   Karstified gypsum in the upper member of the Fatha formation [6].

Fig. 7   Karstified gypsum within the Fatha formation at Atshan anticline, South of Mosul Dam [6].

Fig. 8   Karstified gypsum within the Fatha formation at Atshan anticline, south of Mosul Dam [6].

Fig. 9   Enlarged Google Earth image showing many sinkholes (dark spots encircled by red color), in the upstream area of the dam site [5].
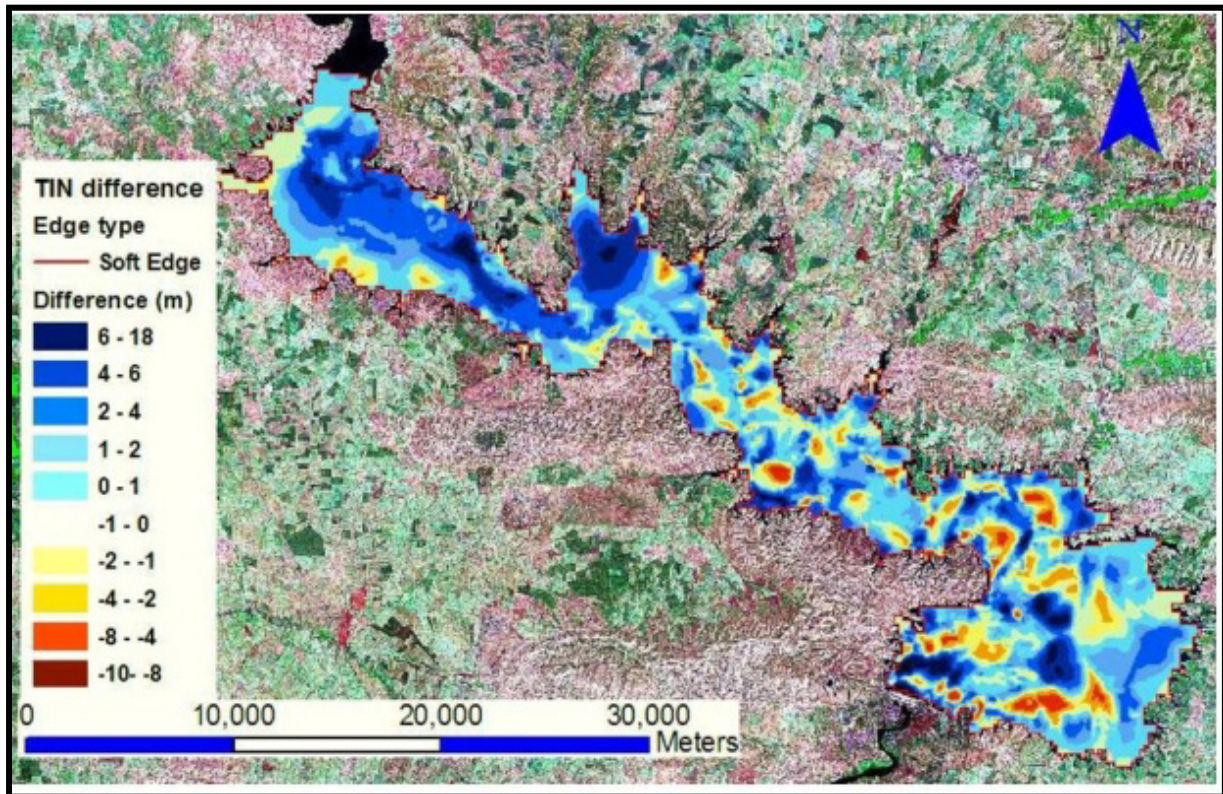
Fig. 10   Results of bathymetric survey of Mosul Dam reservoir carried out in 2011 by a Luleå university PhD student [7].

formation of highly developed conduits and caverns which form easy passages to the flow of ground water and the reservoir water. This had caused extensive dissolution of gypsum and gypsum anhydrite rocks present above and below these limestone layers. These dynamics had caused the collapsing of whole layers of clayey marls and gypsum anhydrite into the underneath cavities forming beds of brecciaed gypsum particles and anhydride blocks embedded into a loose clayey matrix. Four such layers where discovered during the geological investigations and they were termed as the Gypsum-Breccias layers which had thickness ranging between 8 meters and 16 meters. The first layer was found at a depth of 80 meters in the river section and it was marked as the GB0 layer. The other three layers were at higher levels. The last one i.e. the GB3 was discovered at the foundation of spillway chute ski jump. The GB layers proved to be very dangerous due to their erratic behavior during the grouting of the deep grout curtain under the dam. Fig. 11 shows the geological cross section under the dam.

Fig. 12 gives the lithological column under the Mosul Dam central part.

During the excavation works of the spillway chute and flip bucket the GB3 layer was exposed showing spectacular cavities and open joints and cracks. These are shown in the photographs in Fig. 13.

In Fig. 14 the dotted line is the estimated karsts line development in sections 69-87 which is the most problematic area as visualized by the designers, the estimation of this line was based on the results of boring and field permeability testing. The black spots in this figure indicate some of the points of major grout take. Below this line according to the designer's judgment karsts cease to exist and this depth should define the end of the deep grout curtain. The design criteria of the grout curtain, however, called for extending the curtain 20 meters below this line for more safety. In actual fact the depth of dissolution extended below this line after impounding the reservoir. The design criteria and full details of the grouting works are given in Ref. [8].

Fig. 11 Geological long section under dam axis (the long extending from east to west shown has been divided in parts from east to west which are stacked together in the above figure) [4].

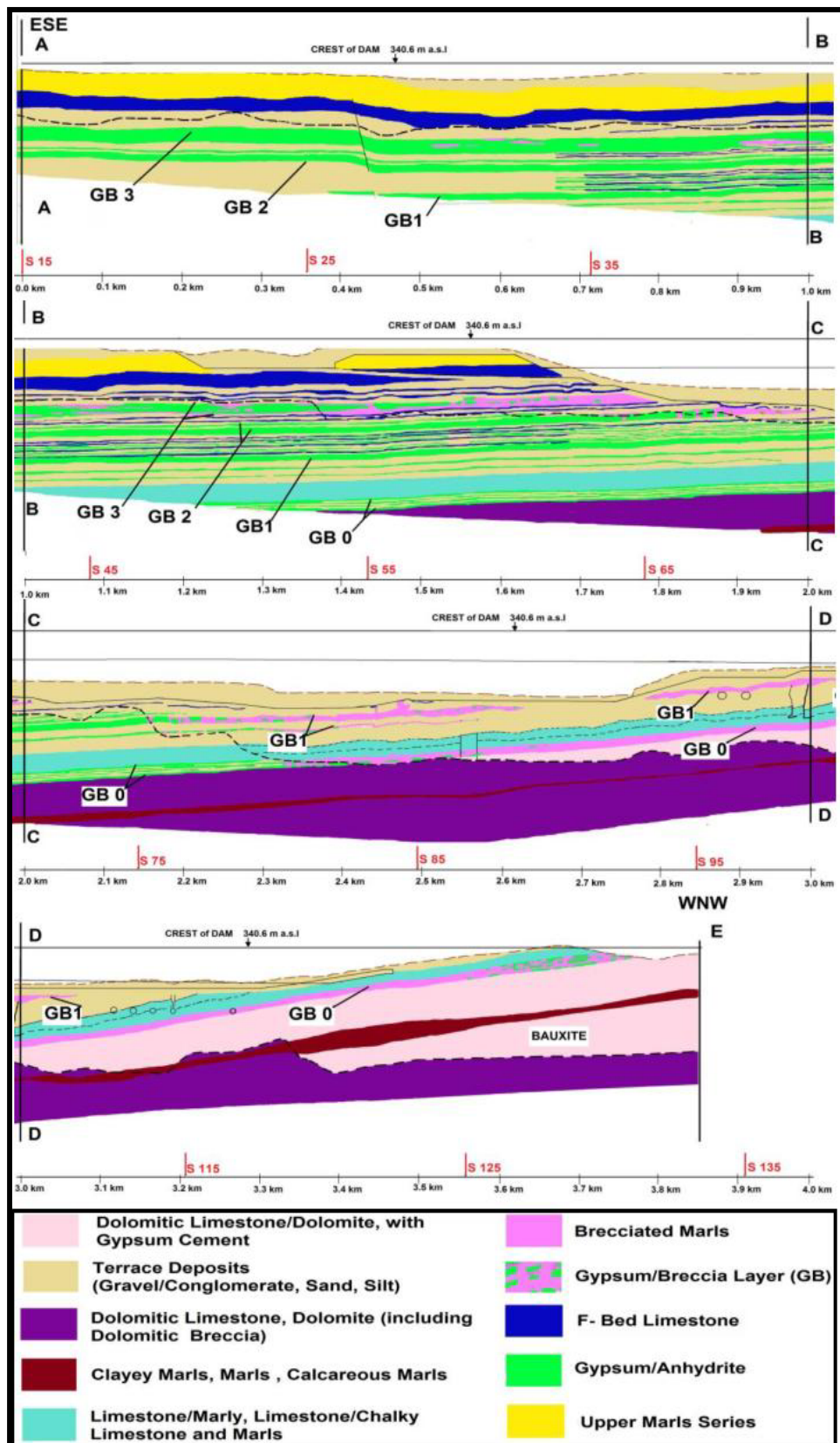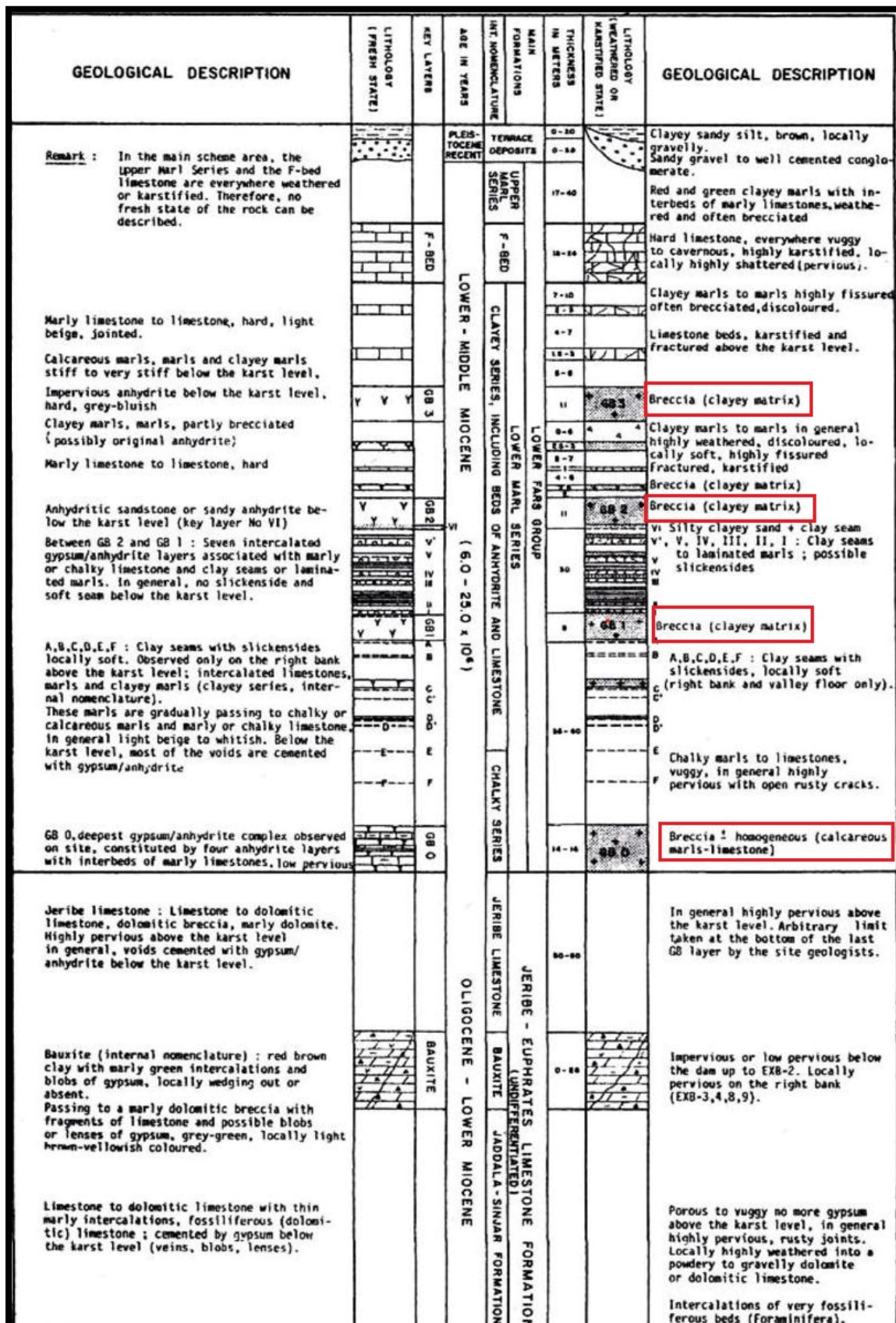| GEOLOGICAL DESCRIPTION	LITHOLOGY (FRESH STATE)	KEY LAYERS	AGE IN YEARS	INT. NOMENCLATURE	MAIN FORMATIONS	THICKNESS IN METERS	LITHOLOGY (WEATHERED OR KARSTIFIED STATE)	GEOLOGICAL DESCRIPTION
Remark: In the main scheme area, the Upper Marl Series and the F-bed limestone are everywhere weathered or karstified. Therefore, no fresh state of the rock can be described.			PLEISTOCENE RECENT	TERRACE DEPOSITS		0-20		Clayey sandy silt, brown, locally gravelly.
						0-10		Sandy gravel to well cemented conglomerate.
					UPPER MARL SERIES	17-40		Red and green clayey marls with interbeds of marly limestones, weathered and often brecciated
		F-BED		F-BED		14-24		Hard limestone, everywhere vuggy to cavernous, highly karstified, locally highly shattered (pervious).
Marly limestone to limestone, hard, light beige, jointed.						7-10		Clayey marls to marls highly fissured often brecciated, discoloured.
Calcareous marls, marls and clayey marls stiff to very stiff below the karst level.						4-7		Limestone beds, karstified and fractured above the karst level.
Impervious anhydrite below the karst level, hard, grey-bluish						10-3		
Clayey marls, marls, partly brecciated (possibly original anhydrite)		GB 3				8-6		
				CLAYEY SERIES, INCLUDING BEDS OF ANHYDRITE AND LIMESTONE	LOWER FARS GROUP	11	GB3	Breccia (clayey matrix)
Marly limestone to limestone, hard						0-6		Clayey marls to marls in general highly weathered, discoloured, locally soft, highly fissured fractured, karstified
Anhydritic sandstone or sandy anhydrite below the karst level (key layer No VI)		GB 2	LOWER - MIDDLE MIOCENE			16-3		
						8-7		
								Breccia (clayey matrix)
Between GB 2 and GB 1: Seven intercalated gypsum/anhydrite layers associated with marly or chalky limestone and clay seams or laminated marls. In general, no slickenside and soft seam below the karst level.		VI V IV III II I	(6.0 - 25.0 x 10⁴)			11	GB 2	Breccia (clayey matrix)
								vi Silty clayey sand + clay seam v', V, IV, III, II, I: Clay seams to laminated marls; possible slickensides
		GB1				50		
A,B,C,D,E,F: Clay seams with slickensides locally soft. Observed only on the right bank above the karst level; intercalated limestones, marls and clayey marls (clayey series, internal nomenclature).		A B C C' D D' E F				8	GB 1	Breccia (clayey matrix)
These marls are gradually passing to chalky or calcareous marls and marly or chalky limestone, in general light beige to whitish. Below the karst level, most of the voids are cemented with gypsum/anhydrite					CHALKY SERIES	54-60		A,B,C,D,E,F: Clay seams with slickensides, locally soft (right bank and valley floor only).
								Chalky marls to limestones, vuggy, in general highly pervious with open rusty cracks.
GB 0, deepest gypsum/anhydrite complex observed on site, constituted by four anhydrite layers with interbeds of marly limestones, low pervious		GB 0				14-16	GB 0	Breccia ± homogeneous (calcareous marls-limestone)
Jeribe limestone: Limestone to dolomitic limestone, dolomitic breccia, marly dolomite. Highly pervious above the karst level in general, voids cemented with gypsum/anhydrite below the karst level.			OLIGOCENE - LOWER MIOCENE	JERIBE LIMESTONE	JERIBE - EUPHRATES LIMESTONE FORMATION (UNDIFFERENTIATED)	50-80		In general highly pervious above the karst level. Arbitrary limit taken at the bottom of the last GB layer by the site geologists.
Bauxite (internal nomenclature): red brown clay with marly green intercalations and blobs of gypsum, locally wedging out or absent. Passing to a marly dolomitic breccia with fragments of limestone and possible blobs or lenses of gypsum, grey-green, locally light brown-yellowish coloured.		BAUXITE		BAUXITE		0-16		Impervious or low pervious below the dam up to EXB-2. Locally pervious on the right bank (EXB-3,4,8,9).
Limestone to dolomitic limestone with thin marly intercalations, fossiliferous (dolomitic) limestone; cemented by gypsum below the karst level (veins, blobs, lenses).				JADDALA-SINJAR FORMATION				Porous to vuggy no more gypsum above the karst level, in general highly pervious, rusty joints. Locally highly weathered into a powdery to gravelly dolomite or dolomitic limestone.
								Intercalations of very fossiliferous beds (Foraminifera).

Fig. 12 The lithological column under the Mosul Dam central part (red rectangles indicate the Gypsum Brescia layers) [4].

Photo 1. Chute area of the spillway, top of GB3 layer; subrounded boulders of gypsum/anhydrite and brecciated marls.

Photo 2. Cavity in GB3 layer.

Photo 3. Open crack in gypsum layer.

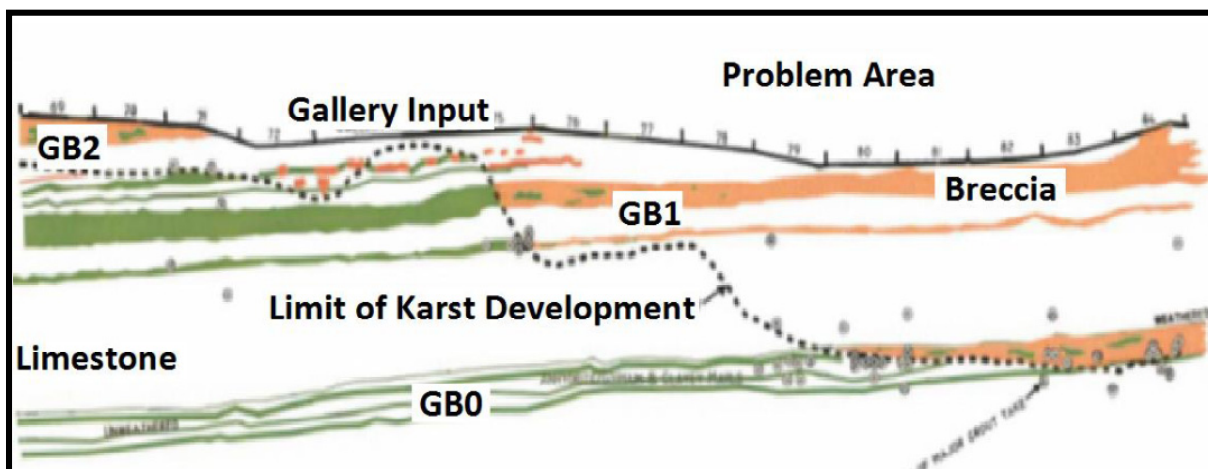**Fig. 13   Cracks and cavities in the GB3 layer below spillway's chute and flip bucket [9].**

Fig. 14   **Estimated karsts line in the problem area (sections 69-87) (The black spots show locations of some of the major grout take locations) [9].**

The schematic diagram Fig. 15 shows the mechanism of the gypsum/breccias layer formation. Groundwater flowing through cavernous limestone can wash the Marley clay from above into cavities already formed in gypsum/anhydrite layers and causing the collapse of more gypsum/anhydrite into these cavities forming continuous layers of the breccias.

The groundwater regime was studied carefully during construction especially in connection with the construction of the pump storage scheme underground cavern structures and the intake/tailrace tunnel. The amount of seepage flow was tremendous and the excavation of the caverns was only possible after performing extensive grouting work all around these caverns in the form of boxes which also served as a protection shells around theme, in addition to driving drainage tunnels all round the caverns. Due to the large amounts of seepage flow the driving of the intake/tailrace tunnel was only possible after grouting the excavation face ahead of excavation work. The quality of seepage water was much different from the river water quality and it contained a much higher concentration of sulfates indicating the passage of water through gypsum and gypsum anhydride layers. Further studies showed that this water belonged to the very large Wadi Der Malih aquifer which is being fed from long distance upstream and which was running below and independently from the river aquifer. This aquifer was also fed directly from the reservoir after impounding. Fig. 16 is a photograph of the water flow of one spring which had erupted during the excavation of the tunnel and could only be stopped after performing much grouting works. The Importance of the Wadi Der Malih aquifer is not only due to the great difficulties it had caused during the construction of the pump storage scheme, but it is also believed it contributed to the formation of a series of sinkholes at the right bank downstream of the main dam as explained later on.

6. Grouting of Gypsiferous Formations (General)

Grouting such formations is very tricky operation. As such grouting begins to seal some seepage paths, this will result in an increase of the hydraulic gradient locally in adjacent parts. Water passing over gypsum becomes chemically saturated within a flow path and in this zone of saturation no further dissolution occurs. As flow continuous, the zone moves downstream and eventually passes from the exit. At this stage, dissolution rates accelerate again sharply. From experience it is known that seepage velocities of 10^{-4} cm/sec in a 2 cm wide gypsum vein, it should dissolve at a rate of few centimeters per year from an advancing front. If the velocities were about 10^{-2} cm/sec gypsum could dissolve at a rate of 9 meter per year. Dissolution
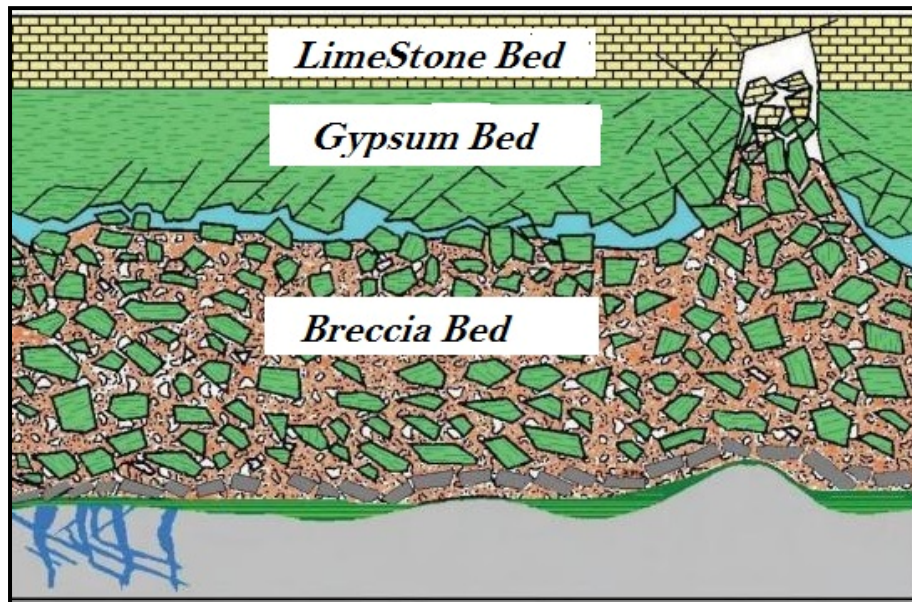
Fig. 15   Schematic diagram showing the formation of a breccias layer.

Fig. 16   The flow (360/sec) from underground aquifer into the intake/tailrace tunnel of the pump storage scheme originating from Wadi Der Malih aquifer [9].

occurs until seepage water reaches a calcium sulfate saturation of 2,000 ppm. Hence the dissolution zone moves downstream as greater quantities of unsaturated water attack a gypsum vein [10, 11].

From this it seems that it is most difficult to seal a cracked or fissured gypsum formation permanently, especially in the presence of other formations which are also jointed, cracked and highly conductive to flow as in the case of Mosul dam foundations especially in view of the very high heads created by the reservoir.

Nevertheless, the designers of the dam considered that grouting should be used as the anti-seepage element for the deep cutoff under the dam, while construction of positive cutoff in the form of concrete diaphragm could have been used instead. A better choice of anti-seepage measure should have been the construction of concrete diaphragm especially that hydro-fraise machines which could go to a depth of 140 m for the construction of such diaphragm were available and the work could have been done from river bed level.

7. The Grouting Works Program

An extensive grouting works program was anticipated by the designers in view of the soluble nature of the foundation and its configuration. One report in 1991 estimated that dissolution intensity at Mosul dam foundations ranged from 42 to 80 tons per day. This process coupled with the presence of karstic limestone and calcareous marls as well as anhydrite presented a very problematic and difficult foundation, which was anticipated by everybody since the beginning, and the consultants and the IBOE (International Board of Expert) which had been appointed to follow the design and construction of the dam agreed the design outlines of the grouting works and their acceptance criteria only after extensive discussions and lengthy meetings.

The first element of grouting works is the contact blanket grouting covering the contact area of the clay core with the foundation surface to close all preferential seepage paths by filling all fissures and joints and protect from concentrated seepage flows directly under the core. The second is the deep three rows curtain which extends down to the karst line.

A concrete grouting gallery was constructed at the bottom of the cutoff trench so as to continue the grout curtain works without interfering with the embankment construction. It was also meant to be used for continuous observation of the curtain performance during operation. Pairs of open pipe piezometers were installed upstream and downstream of the curtain, one pair at each section of the gallery in order to be able to measure the efficiency of the curtain. The gallery proved to be of immense usefulness to carry out maintenance grouting of the curtain in what was to be defined as massive grouting, a process which has continued from the first filling of the reservoir up to now. The required efficiency of the grout works was to reduce the seepage flow to safe limits to allow the water upstream the curtain to be saturated with calcium sulfate and therefore stopping any further dissolution of gypsum or t hydration of anhydrites. In the limestone beds grouting was to plug and seal all anticipated cracks and joints and hinder the free flow of seepage. The criteria were expressed in terms of Lugeon units of rock mass permeability values which were defined specifically for each of the blanket grouting, and the various depth and parts of the grout curtain. During the progress of the work it was evident that while cracks and cavities in limestone could be reasonably filled, the criteria could not be achieved over many locations in the GB beds in the deep curtain at depth which remained open to seepage and were described at the time as windows. These windows remained open in many locations under the central part of the dam even after the full scale impounding of the reservoir had started in the spring of 1985 when the grouting problem was not yet settled; a thing which could not be stopped due to the early closure of the river in October 1984.

The beds where this problem had severely occurred were the breccias aforementioned which proved very difficult to grout, and if temporarily sealed they opened again to the flow after the dispersion of the grout mix within the loose matrix. This situation led later on to accelerated dissolution and formation of large cavities during the lifetime of the dam.

In spite of the many grouting techniques that were tried to solve this problem including changing grout mix designs and using different pressures, the problem persisted and even the use of chemical grouting with different solutions was equally unsuccessful [8].

8. Problems Encountered during First Filling of the Reservoir (1985-1988)

The first filling uncovered many serious problems requiring much serious attention and studies and resulted in remedial works. All is summarized in the following:

8.1 Seepage Springs in Left Bank

As water level in the reservoir increased many springs began to develop in this bank. The more serious once were close to the right and left sides of the spillway bucket structure and chute and others were at further left. The seepage water was collected for measurement and chemical testing. The total quantity of seepage was 830 l /second (on 22nd March 1986)

which corresponded with a reservoir level of 304 masl. This could yield, if extrapolated to 2 cubic meters per second at full reservoir elevation of 330 masl. Chemical tests showed an increase in salts content indicating leaching of gypsum at a rate of 30 tons/day. This is equivalent to void volume of 10-15 cubic meters. Fig. 17 shows the obtained test results of water seepage from the most important five springs as the water level was raised during the period February-August 1986 [12].

Further hydro geological investigations by installing more open pipe piezometers and use of tracers to discover seepage paths showed the need for extending the depth of the grout curtain at certain sections and adding another line of grouting holes in others. Arrangements were made to catch some springs by pipes to discharge away the water safely and others were covered by filter material. Anew deep curtain was also constructed along the left side of the spillway's chute to stop seepages flowing underneath the chute and across it from the upstream direction. An extension to the left bank grout curtain along dam axis was performed also to protect the left bank from being outflanked by water seeping around the executed curtain.

Although these additional works reduced the amount of seepage and the dissolution of gypsum, they could not eliminate them.
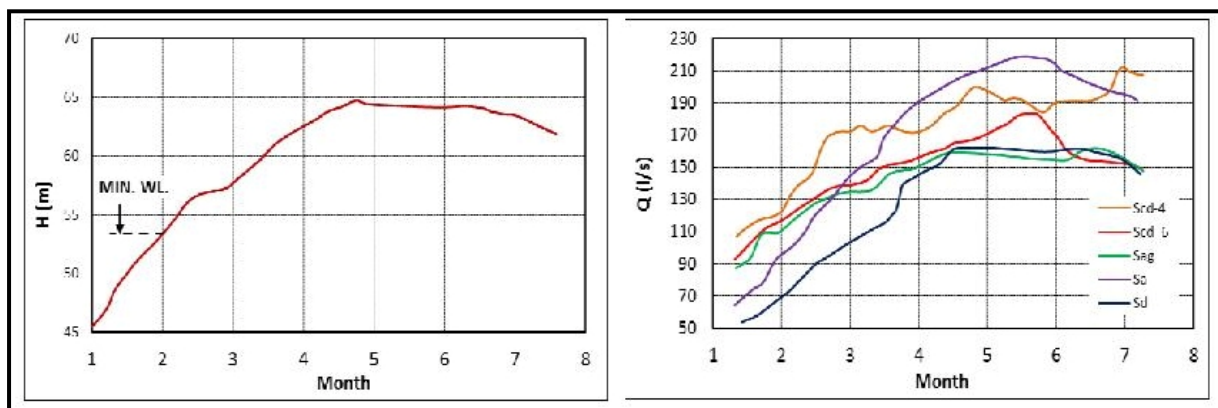

Fig. 17   Chemical test results of water seepage from the most important five springs vs. water level was raised during the period February-August 1986 [12].

8.2 Deterioration of the Grout Curtain under Main Dam

Similar measurements of seepage water quantity and quality from under the dam at the river channel section, which was collected from the pond created by the coffer dam no 6 used during river diversion, showed alarming dissolution of gypsum and increased transmissibility during the same period [12], as indicated in Fig. 18.

The increase in seepage quantity was accompanied by reduction of the grout curtain efficiencies in many sections in the river channel and could be attributed to the increased size of the aforementioned windows due to increased dissolution. Grout curtain efficiencies at various parts were measured by observing the difference in the hydraulic head between the upstream and downstream piezometers that were installed in pairs in the grouting gallery. These piezometers were and still are up till today as the only means to discover the formation of cavities in the foundation and to indicate the need for filling grouting as a maintenance procedure.

As water level was reaching higher elevations the formation of large cavities was posing a constant threat to the stability of the dam. This required the introduction of introducing a new technique which was called (Massive Grouting) to inject thick grout (by

adding 3 weight sand to 1 weight cement, 4% of bentonite that needed to be activated using sodium carbonate using 1:1 water/cement ratio). It also required the fast transport of the grout mix in dry conditions by truck mixers to the location of three deep boreholes lined with steel pipes that penetrated the core from the crest of dam to the gallery, where it was mixed and injected in the required treatment zones. This operation known as "Massive Grouting" continued from 1986 up to the present days in addition to other forms of conventional grouting as needed. The use of this procedure is probably a unique case in the whole world. Grouting records shows that the quantity of injected grouting from 1986 up to and including 1988 was 25,000 tons of injected solids out of which 12,200 tons are of massive grouting and even larger quantities were pumped in the following years [8].

8.3 Development of Sinkholes

In September 1986 an inspection of the right rim of the reservoir was carried out when the water level had been drawn down to EL.316.4m from El.309m which it reached during the previous flood season. This inspection revealed the development of a series of sinkholes at the right bank at many points at about 150 meters from the contact of the dam with the right abutment. One sinkhole of major proportions was located also at about 1 kilometer or so away. These
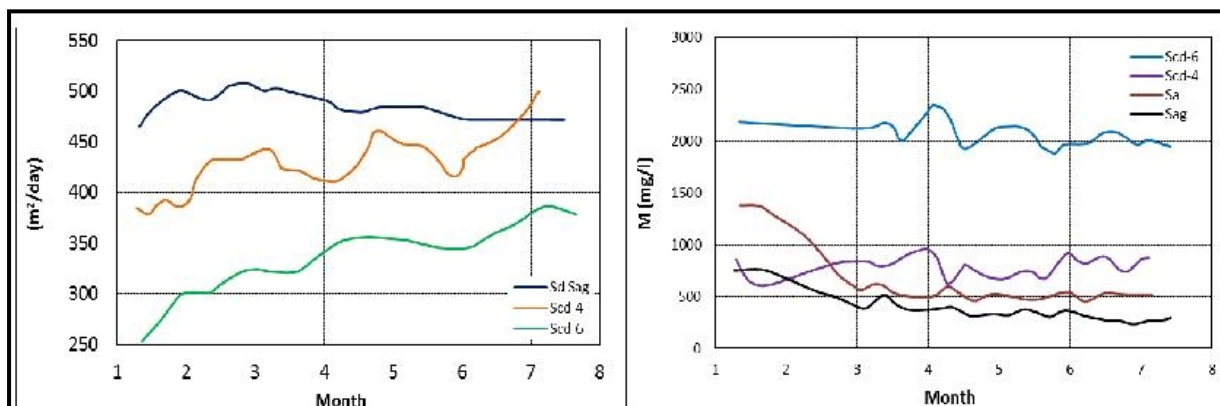

Fig. 18   Increased transmissibility vs. time (February-August 1986), and continuous dissolution of gypsum in the same period for the increased head shown in Fig. 17. (Dissolution had leveled off after the initial increase in the first three months which was due to the washing away of gypsum particles fillings in the cracks and joints of the rock formation) [12].

sinkholes showed dramatic solution of the gypsum layers which were exposed on the shore line. During the operation years of the dam and specifically from 1991 to 1998 new series of sinkholes began to form in the downstream area of the dam. These sinkholes followed a straight line alignment parallel to the axis of the dam and at about 400 meters away. These sinkholes were indication of an active process of rock dissolution. Careful observations and measurements indicated that the ground surfaces at the sinkholes locations had settled gradually and collapsed in enlarged underground cavities which were formed partly by the fluctuation of the water level resulting from the operation of the reregulating dam 8 kilometers to the south of the main dam and partly due to the connection to Der Maleh underground aquifer which runs under the dam area and being charged from the right rim of the reservoir through the gypsum layers day lighting at the right rim. The location of these sinkholes is shown in Fig. 19, and the photographs of sinkhole (SD2) given in Fig. 20 show the initial phase of its formation in the

contractor's concrete paved work area and the final shape after full development.

The chemical composition of the water in the sinkhole gave the same results as those from Der Maleh aquifer encountered during the excavation of the pump storage scheme tailrace tunnel not very far from the sinkholes location. Further from this area on the same alignment at the river bank one spring was discovered after the erosion of the alluvium cover due to spillway operation. This spring seems to follow the same sinkhole phenomena and its water has same composition of Der Maleh aquifer (Fig. 21).

By contrast to the right bank sinkholes which began by ground surface cracking followed by ground surface settlement until the occurrence of the full collapse, one sinkhole at the left bank very close downstream of the dam of dam shown in Fig. 22 occurred suddenly in February 2002 without previous warning. It was situated close to housing colony 150 meters downstream of the left flank
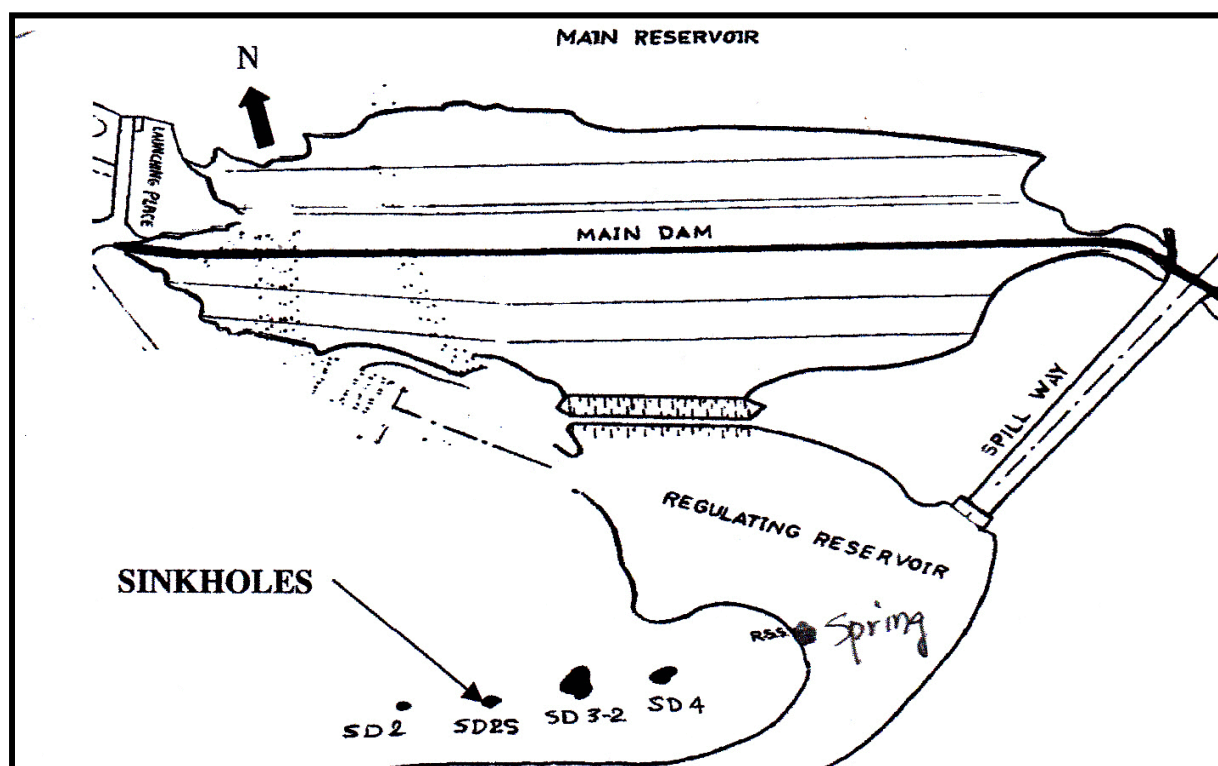
In Fig. 23, this sinkhole seems to be located on the

Fig. 19   Location of downstream sinkholes which had developed during the period [9].

Fig. 20   Two views of sinkhole SD2 at the initial stage and final stages of development [9].
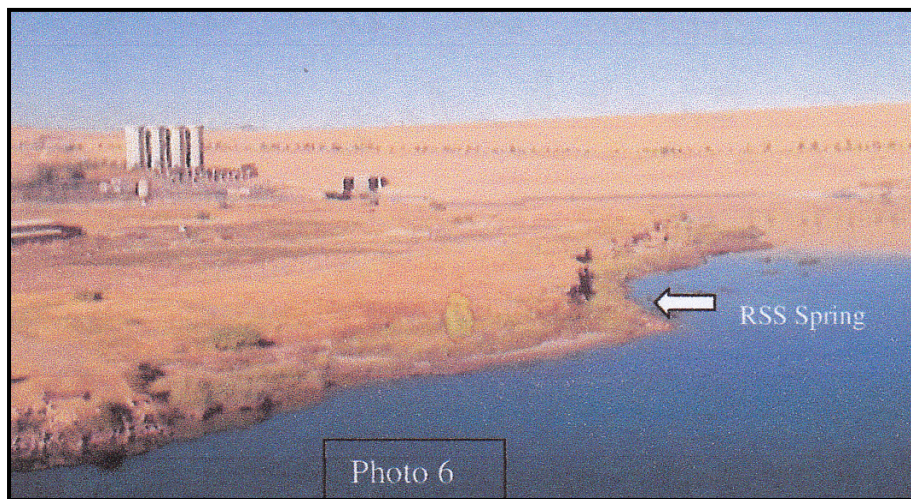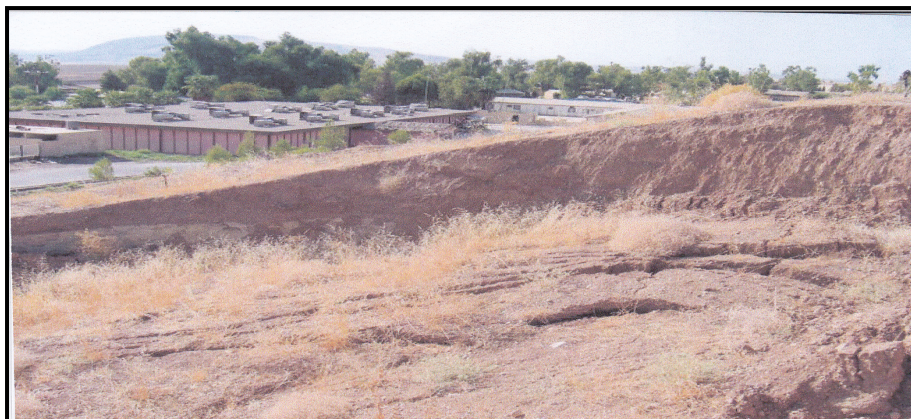

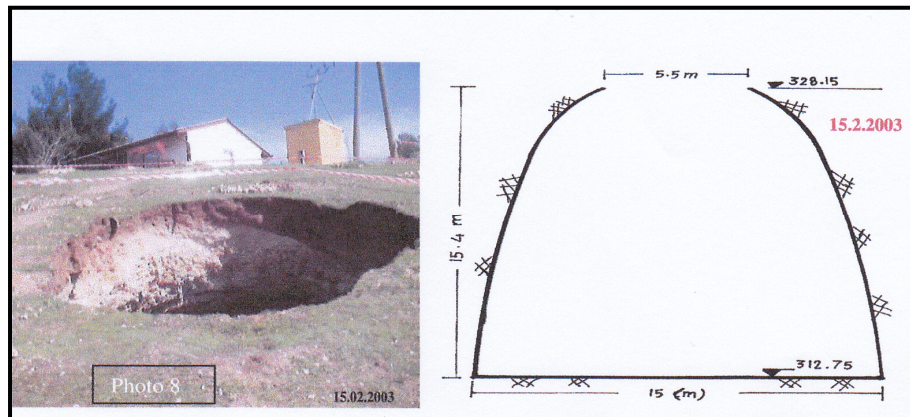**Fig. 21   Spring downstream of dam [9].**

Fig. 22 Photographs of the right bank sinkhole showing development stages and sketch indicating mapped dimensions [9].
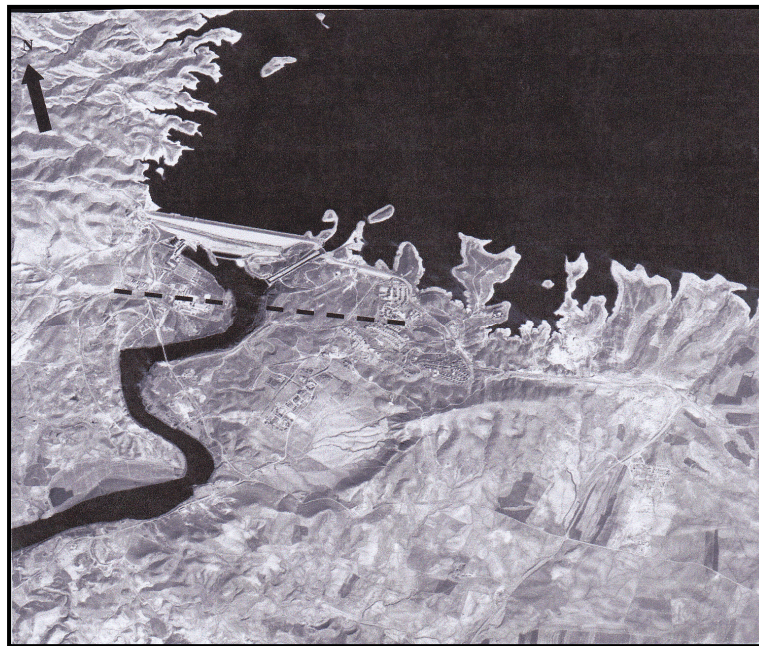

Fig. 23 Aerial view of the Dam area showing alignment of downstream sinkholes [9].

same line of the other sinkholes on the right bank .One suggestion to the sudden collapse of this sinkholes is the possible infiltration of

9. Mosul Dam Flood Wave Study and the Question of Badush Dam

In early 1984, the Ministry felt the need to assess the possible damage that could be incurred as result from Mosul Dam failure and the subsequent flood wave released in the Tigris River valley. So it signed a contract with the same consultant of Mosul dam to do such study. The study being done, and the report being ready in 1985 showed the colossal damages that could

result in such an event to both human lives and material properties and infrastructures with its impact reaching beyond Baghdad. The main conclusions of the study showed that: (1) if failure would occur at all, the most probable cause would be the foundation geology; (2) for the various scenarios of the reservoir water levels at failure, the initial wave hydrograph would be as shown in Table 2, with peak discharge of 551,000 cumecs can be expected (Scenario A); (3) the calculated travel times to various cities on the river, max height of wave, and flooded areas are shown in Table 2 and Fig. 24 [13].

These alarming results prompted the Ministry of

Table 2   Flood wave hydrograph at various initial conditions of failure.

Hours/Case	A	B	C	D
0	1	1	1	1
1	13	13	13	13
1.5	80	80	80	80
2.0	215	210	215	212
2.5	372	356	335	325
3.0	474	452	422	404
3.5	535	499	480	453
4.0	551	510	509	475
4.5	538	469	497	460
5.0	507	469	497	460
6.0	405	382	435	405
8.0	271	266	186	278
10.0	186	192	195	198
12.0	123	136	130	142
18.0	37	47	39	49
24.0	18	2	19	22

Table 3   Flood wave discharge, time of arrival and flooded areas at various locations in the Tigris River Valley.

| Location	Discharge (m^3/sec)	Time of arrival (hr)	Wave height (m)	Distance (km)	Flood area (Km^2)
Dam site	551,000		54	0	
Regulating Dam	545,000	1.3	48	9	
Eski Mosul	481.000	1.6	45	17	
Mosul City	405,000	4	24	69	74.044
Hamam Ali	370,000	5	18	97	
Tikrit	185,000	22	15	422	68.985
Sammara	162,000	25	10	479	30.100
Balad	115,000	28	9	516	
Khalis	81,000	31	6	566	
Tarmiya	72,000	33	4	597	
Baghdad (North)	46,000	38	4	638	
Baghdad (Center)	35,000	44	4	653	216.934
Baghdad (South)	34,000	48	3.5	674	
Diyala Confluence	34,000	>48	3	685	
Salman Pak	31,000	>48	3	708	
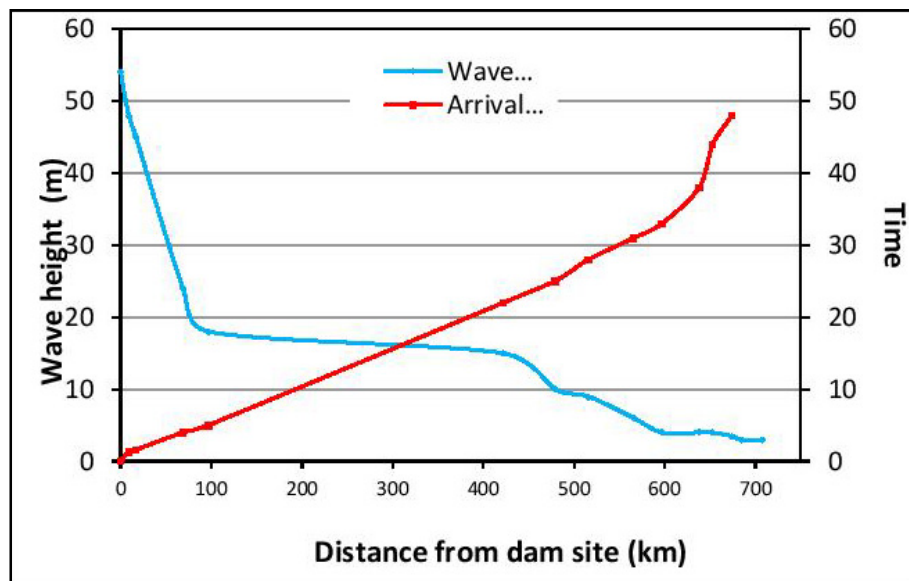
Fig. 24 Wave height at various distances downstream of dam and time of travel time of arrival.

Irrigation, when it was clear that the dam presented a grave hazard on the population, to design and start construction of a protective dam 40 km downstream from Mosul Dam to contain the full volume of Mosul Dam flood wave in case of its failure. This is the dam called Badush Dam which is probably a unique case of this size in the history of dam construction. Unfortunately the works were suspended in 1991 after completing 30-40% of the works, which was due to the UN economic sanctions imposed on Iraq after its invasion of Kuwait.

10. Safety Evaluation of the Dam

10.1 Evaluation of the Dam Safety Conditions in 1988

From the beginning of the detailed design phase until the completion of Mosul Dam, it was followed closely by the International Board of Experts appointed by the Owner; the Ministry of Irrigation; later the Ministry of water resources. This Board helped tremendously in reaching safe and sound design and construction of the dam. The Board however did not have any saying in the final selection of the dam site which was done previously by others, nor of selecting positive concrete diaphragm for anti-seepage measure instead of grouting, as the last detailed geological investigation works were not ready when the Consultant had their

preliminary planning report approved by the Owner. But the Board recognized the problem of gypsum in the foundation and gave early warnings and all necessary advice to refine the grouting criteria; it stopped, short however, from reaching the design criteria required to seal the brecciaed gypsum in the foundations once and for all, these breccias beds are recognized now not to accept any form of grouting. The dam as completed was considered by the dam as safe from in all aspects except for its foundation. The conclusion reached in 1988 by both the Board and Consultant at the completion and operation of the dam was that grouting treatment works, massive and conventional, should continue for the whole life of the dam. This conclusion was supported by training an Iraqi grouting team by the contractor at the urging of both the board and Consultant to fulfill this task. This team was successful in treating many grave cases of very large dissolution cavities, of which the case of one that took 5,000 tons of solid grouting materials is well documented.

10.2 Evaluation of the Dam Safety Conditions in 1995

No general review of the dam safety was carried out until 1995. A general inspection of the dam and a review of all the accumulated data and all available reports and measurements were conducted by two

Bulgarian Specialists. They judged that the dam condition was generally acceptable, but they recommended taking the actions which are summarized in Table 3.

10.3 Evaluation of the Dam Safety Conditions in 2004-2005

After the 2003 war, and the occupation of Iraq by the United State and Britain, the US army corps of engineers performed a quick survey and a safety of Iraq dams and concluded that Mosul Dam was in a precarious state and formed severe threats on the occupation forces stationed in the Tigris River Valley. A complete safety assessment study was then initiated in which Washington group International & Black and Veatch (JV) were contracted in 2004 to do. Their report was submitted in August 2005 and included the results of thorough investigation of the dam conditions; it even included the assessment the dam safety conditions that was carried out by a PoE (panel of experts) which was formed especially to carry out this task. The panel assessment was based on potential FMA (failure mode analysis) and recognizing the usefulness of Badush Dam.

The PoE summary of the findings included the following main points:

(1) Construction of Badush Dam between Mosul Dam and the City of Mosul would address downstream loss-of-life risks for all possible positional failure modes.

(2) Construction of a diaphragm wall from the crest of the dam using current technology is an unproven alternative that could not, therefore, be relied upon to reduce loss-of-life risk sufficiently, considering the very large downstream population-at-risk. In addition, this alternative would be more costly than building Badush Dam.

(3) Construction of an upstream diaphragm cutoff wall and upstream impermeable face might reduce loss-of-life risk sufficiently, however, it would require an extended reservoir lowering and it would be more costly than building Badush Dam.

(4) Foundation grouting does not provide acceptable long term loss-of-life risk reduction, considering the very large downstream population at risk.

(5) Continued and improved foundation grouting and careful monitoring and visual inspection would be reasonable risk reduction measures to extend the economic benefits of the Mosul Dam (power generation and irrigation) as long as practical

From the above it is clear that the PoE recommends the necessity for continuing the maintenance grouting works, the usefulness of Badush dam, but it rules out the use of diaphragm wall as a replacement of the grout curtain. It is worth mentioning that the diaphragm alternative was proposed in 1987 by two consultants during construction and that it was rejected by the International Board of Experts of the Dam.

Table 3   Summary of recommended actions.

	Item examined	Recommended action
1	State of gypsum dissolution	Continue the grouting programs as before as maintenance work for the whole life of the dam and never atop
2	Deep grout curtain	Breadth of curtain is not sufficient according to Soviet and Bulgarian standards. Add two more grouting rows, one at each of the U/s and D/S of existing curtain
3	Instrumentation	Readings were judged acceptable, no action is required except routine maintenance
4	Seepage and dissolved salts quantities	The quantities of these seem to increase with rising water level of reservoir, so it is recommended not to accumulate water above Maximum Operation Water Level (EL. 330 masl). If such event occurs in the event of very high floods, then the reservoir is to be drawn down immediately below this level. WL should not be kept for appreciable length of time at this level in any event
5	Ground water measurement at downstream	Many more open pipe piezometers should be installed at the near vicinity of the dam at the downstream. I is most important to observe ground water movement there and relate this to reservoir water level fluctuation

10.4 Evaluation of the Dam Safety Conditions in 2006-2007

A new PoE was formed by the Ministry of Water Resources in 2006 to follow up the dam safety question. This PoE was formed mainly from Engineers from Harza Engineering (USA) and one member from Italy; but it shall be referred to as the (Harza PoE). The PoE had a series of meeting extending over 2006 and 2007. The main worries of this PoE were about the seepage under the dam and the possibility of the formation of new sinkholes; this was highlighted by the formation of the sinkhole on the left bank very close to the dam in 2002 (Fig. 22). During these meetings the following conclusions and recommendations were forwarded:

(1) The dam safety was questionable even with the continuation of the maintenance grouting program.

(2) There was g a very high possibility of the occurrence of sinkholes on the left bank close to the dam body.

(3) The need for intensive new geophysical investigation to be carried out using Geo-Radar in addition to the other conventional investigation that was ongoing at the time.

(4) Install many more open pipe piezometers at this bank to observe ground water movement and give early warning of the formation of new sinkholes and take action by emptying the reservoir.

(5) Limit the maximum operation level of the reservoir to (319 masl) instead of the maximum designed operation water level of 330 masl.

(6) Construct a positive cut-off in the form of concrete diaphragm as a permanent solution as the protracted grouting had not been sufficient to stabilize the situation. Admitting that such a cut-off would have unprecedented depth, therefore its implementation should be studied by uniquely specialized contractors and equipment manufacturers.

(7) The PoE went further to cast doubts on the usefulness of Badush Dam stating that the current design of the clay core may not be sufficient to sustain

the Mosul Dam flood wave and that the bottom outlets may get clogged by debris leading to overtopping of the dam.

While the limitation of the reservoir water level was enforced during the subsequent years the question of the diaphragm was not settled and maintenance grouting work was continuous by the site crew as previously done until June 2014 when the Mosul City fell to ISIS terrorists. Even the dam site was captured by them but only for 20 days before they were repelled back by government and coalition forces. However the grouting works activities as the crew left and did not go back to site again.

10.5 Evaluation of the Dam Safety Conditions in 2015-2016

The repercussions of the halting of the grouting maintenance work was visualized and sensed sharply by USACE who were very much aware of the fragile situation of the dam foundation and their reaction to this was prompt. An interagency team from many United States agencies was formed in the beginning of 2015 which was lead by the USACE to carry out measurements, surveys and observations to follow developments that might lead to the dam failure. The following was done: (1) An early warning system consisting of remote sensing instruments was installed to check for movement and settlement in important locations on the embankment and structures; (2) Installing observation cameras on the dam crest and downstream berms for the same purpose; (3) A bathymetric survey upstream and downstream of the dam was conducted by socialized divers.

The findings of the US interagency team were alarming and may be summarized in the following:

(1) There were signs of increased formation of caverns and sinkholes under the dam. The discontinuation of grouting works from August 2014 until beginning of 2016 has resulted in an increased loss of gypsum and formation of new cavities of about

10,000 cubic meters more than what normally would have happened with the continuation of grouting shown in Fig. 25.

(2) Increased concentration of sulfates in the seepage water was measured indicating increased dissolution of gypsum.

(3) Signs of increased monolith movement in the grouting gallery and cracks opening were observed and measured. It was concluded that they were direct results of settlement in the gallery and hence in the foundations. The cumulative record of settlement in the grouting gallery which was kept from 1986 and extended to the end of 2015 showed sharp increase in settlement in the last year which indicates a worsening situation in the dam foundations.

(4) A SPRA (screening portfolio risk analysis) was performed to obtain the relative risks imposed by Mosul Dam relative to large dams in USA. The screening process considered loading frequency, an engineering rating to estimate a relative probability of failure, and both human life loss and economic. The evaluated risk results were compared to the risks in a total of 563 dams and 108 other with separate consequence structures which belonged to the USACE portfolio of dams. This ranking showed Mosul Dam to be in a state of extreme relative risk as shown in Fig. 27. In fact it shows that Mosul Dam is in a state of extreme and unprecedentedly high relative risk.

The US Interagency Team concludes its report by the following statement shown in Fig. 28.
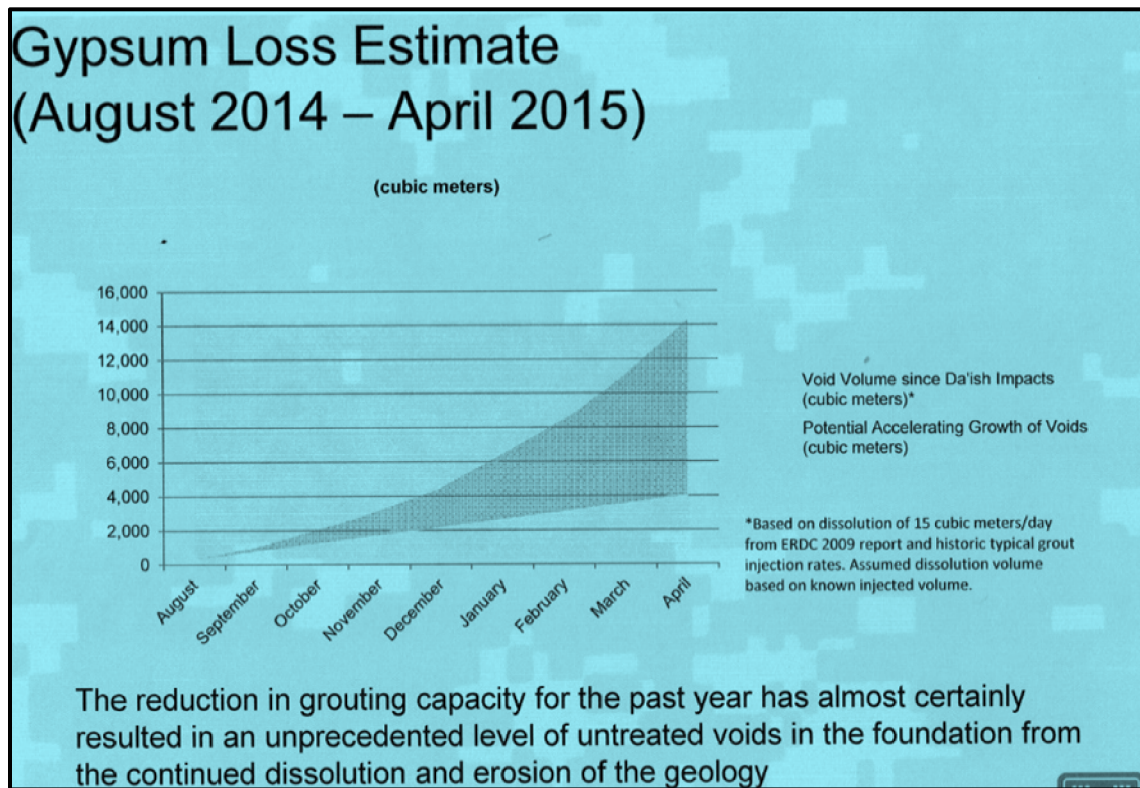

Fig. 25 Dissolution of gypsum without grouting (lower curve: estimated and without grouting; upper curve: measured) for the period (August 2014-April 2015).
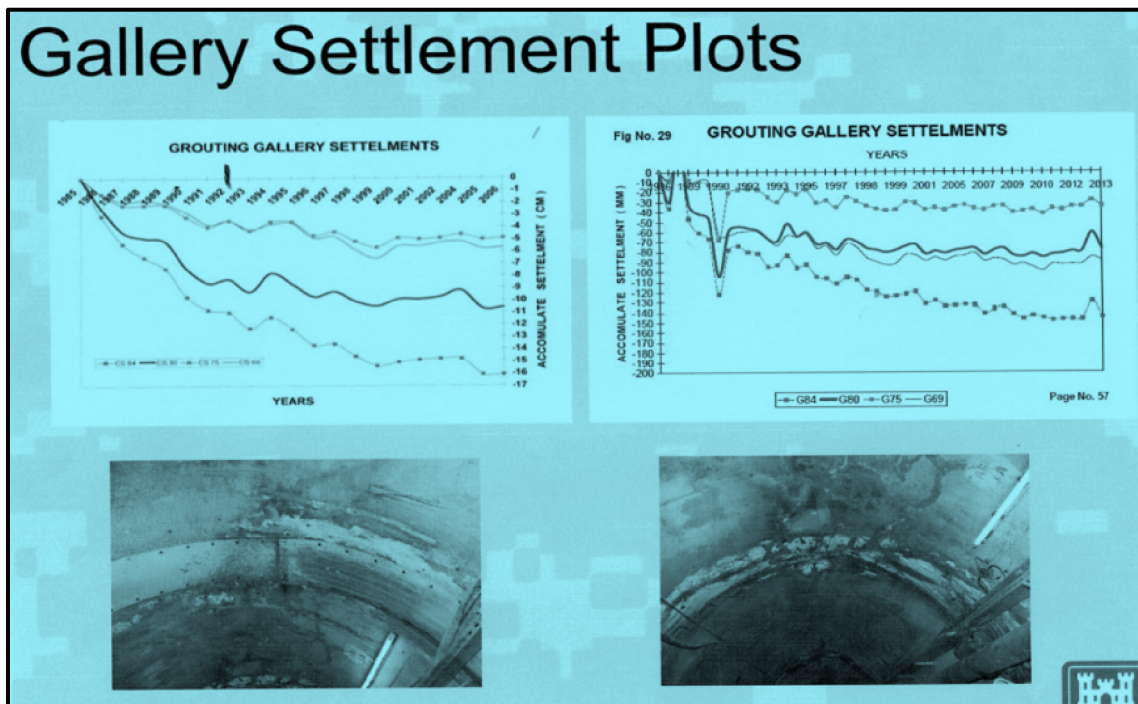
Fig. 26   Cumulative settlements in the grouting gallery recorded in sections 69, 75, 80, and 84 from 1986 till end of 2015.
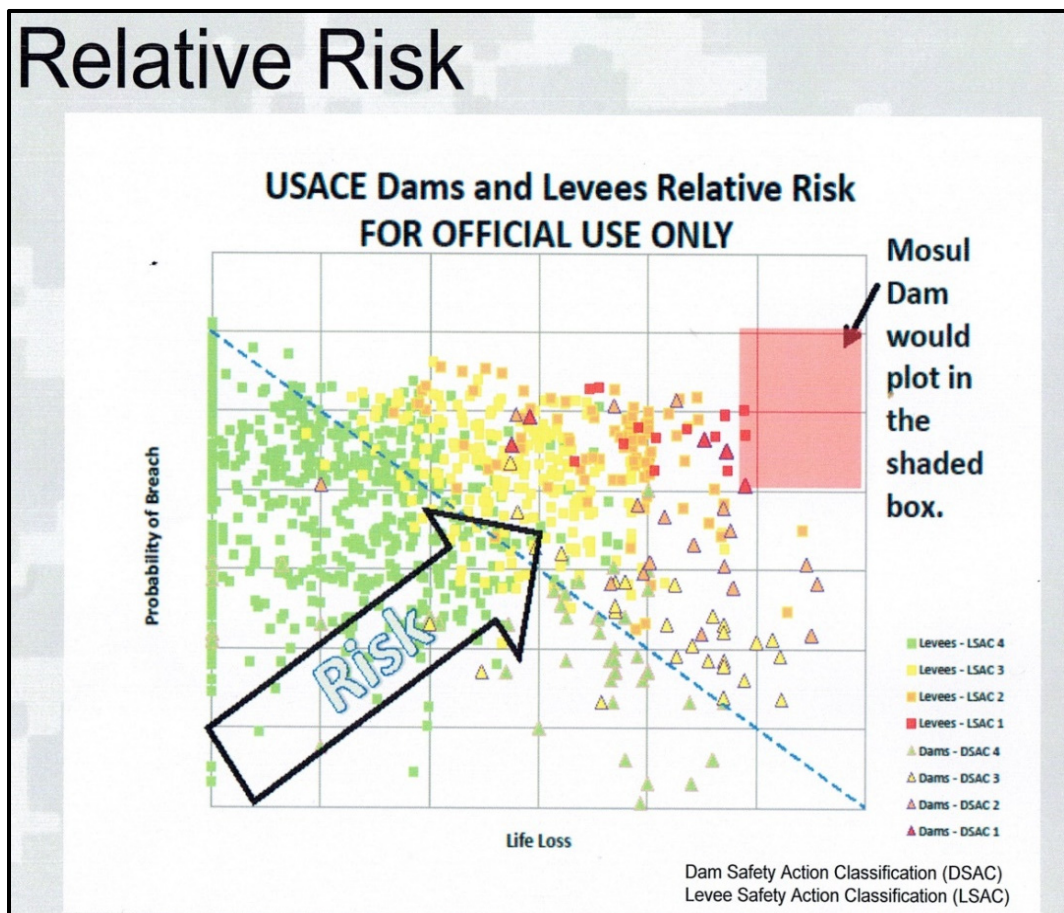

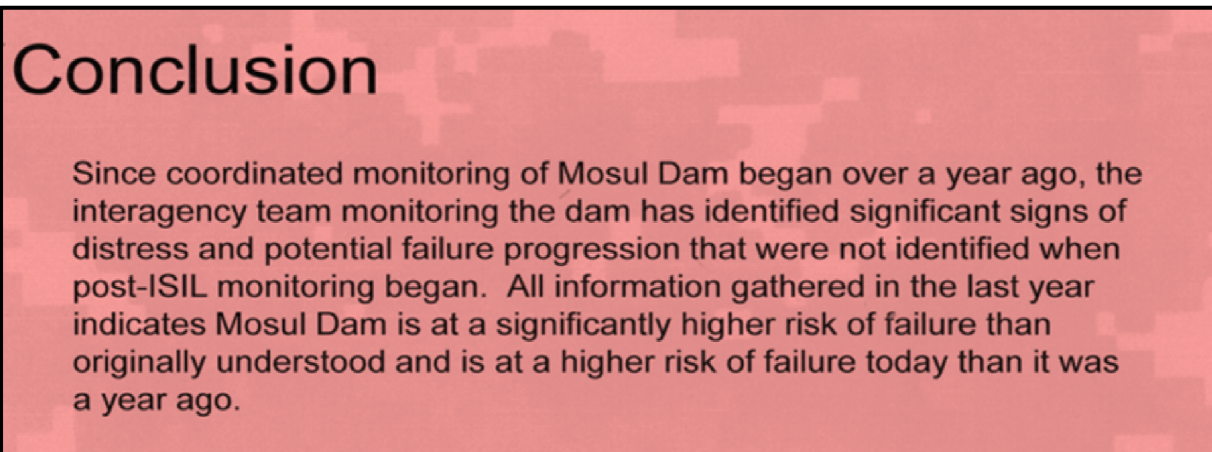**Fig. 27   Plot showing the severe relative risk of Mosul Dam.**

Fig. 28   US interagency report conclusion.

11. Present Situation and Final Remarks

The safety condition of Mosul Dam justifies its description of "The Most Dangerous Dam in the World" [14, 15]. A study of the dam break flood wave was carried out by the JRC (Joint Research Centre) of the European Commission and issued its report issued the report of a study which was carried out in April 2016. This study showed that the number of affected people can reach up to 6,248,000 and can inundate an area of 7,202 square kilometers. Apart from the immediate losses of lives and material properties and infra structure, stagnant water can remain over these areas for as long as 12 days. Such water polluted with disintegrated human and animal corpses and mixed with sludge and sewer water can cause the spreading of infectious diseases of various sorts [16].

With such grave consequences, the Iraqi government was pressured by the USA government to conclude a multibillion dollar contract with an Italian firm, which was to be financed by the World Bank. The objectives were to carry out an enhanced grouting program employing modern equipment's and digital observation and recording system enabling enhanced follow up, in addition to training an Iraqi crew in carrying out the work in the future.

The works of this contract have been done under the supervision of the USACE and the participation of Iraq engineers. The works are coming to a close next July and the Iraqi crew will continue these works.

Recent word from the site gives an optimistic evaluation of the conditions at the site at the present, but the question that remains without answer is what could happen in the future, and whether driving a diaphragm or construction of Badush Dam will be pursued. One thing remains for sure; the continual replacement of parent rock in Mosul dam foundation by weaker grouting materials will not result in better conditions than the first days of dam operation, nor will it contribute to lower possibilities of sinkholes formations. The dam will continue to pose a threat to Iraq even with continuous grouting [17] and this must be pondered by the Iraqi policy makers in any future planning regarding the dam. The dam should be decommissioned sometime in the future or a permanent solution other than grouting must be pursued.

References

[1]   Adamo, N., and Al-Ansari, N. 2016. "Mosul Dam the Full Story: Engineering Problems." *Journal of Earth Science and Geotechnical Engineering* 6 (3): 213-44.

[2]   Adamo, N. 2014. "Mosul Dam: The Most Dangerous Dam in the World." Lecture delivered to PhD students audience in Lålue Technical University on 10th November 2014.

[3]   Adamo, N., Al-Ansari, N., Issa, E. I., Sissakian, V., and Knutsson, S. 2015. "Mystery of Mosul Dam the Dangerous Dam in the World: Problems Encountered during and after Impounding the Reservoir." *Journal of Earth Science and Geotechnical Engineering* 5 (3): 47-58.

[4]   Swiss Consultants. 1979. *Mosul Dam Project Planning*

Report. The State Organization for Dams and Reservoirs, the Ministry of Irrigation, Iraq.

[5] Sissakian, V., Al-Ansari, N., Issa, E. I., Adamo, N., and Knutsson, S. 2015. "Mystery of Mosul Dam the Dangerous Dam in the World: General Geology." *Journal of Earth Science and Geotechnical Engineering* 5 (3): 1-13.

[6] Sissakian, K, Adamo, N, Al-Ansari, N, Knutsson, S, and Laue, J. 2018. "Badush Dam, NW Iraq; A Geological Study." *Journal of Earth Science and Geotechnical Engineering* 8 (2): 1-15.

[7] Issa, E. I., Al-Ansari, N., and Knutsson, S. 2013. "Changes in Bed Morphology of Mosul Dam Reservoir." *J. Advanced Science and Engineering Research* 3 (2): 86-95.

[8] Adamo, N., and Al-Ansari, N. 2016. "Mosul Dam the Full Story: Engineering Problems." *Journal of Earth Sciences and Geotechnical Engineering* 6 (3): 213-44.

[9] Washington Group International, Black and Veatch J. V. 2005. *Mosul Dam Study.* Final Report, Task Order No. 8. Republic of Iraq Project Contracting Office, Provisional Coalition Authority.

[10] James, A. N., and Kirkpatrick, I. M. 1980. "Design of Foundations of Dams Containing Soluble Rock and Solis." *Quarterly Journal of Engineering Geology and Hydrogeology* 13: 189-98.

[11] Morrison-Knudson Inc. 1989. *Solution Equilibrium and Kinetic Rate Studies.* Unpublished report.

[12] Guzina, B., Sarić, J., and Petrovic, N. 1991. "Seepage and Dissolution at Foundation of a Dam during the First Impounding of Reservoir." Paper presented on ICOLD Meeting, Vienna, Austria.

[13] Swiss Consultants. 1984. *Mosul Dam Flood Wave Study Report* (Vols. 1-3). Security measures II, Addendum 3, Task 2. Confidential report submitted to the Ministry of Irrigation, Republic of Iraq.

[14] Adamo, N., and Al-Ansari, N. 2016. "Mosul Dam the Full Story: Safety Evaluations of Mosul Dam." Journal of Earth Science and Geotechnical Engineering 6 (3): 185-212.

[15] The Japan Times, News. 2016. "Most Dangerous Dam Facing Collapse, Threatens Half in Mosul: Us Army." February 10th, https://www.japantimes.co.jp/news/2016/02/10/world/dangerous-dam-facing-collapse-threatens-half-million-mosul-u-s-army/#.XII8ECJKjZ4.

[16] Annunziato, A., Andredakis, I., and Probst, P. 2016. *Impact of Flood by a Possible Failure of the Mosul Dam, Version 2.* JRC technical reports. EU Commission. http://publications.jrc.ec.europa.eu/repository/bitstream/JRC101555/lbna27923enn.pdf.

[17] Kelley, J. R., Wakeley, L. D., Broadfoot, S.W., Pearson, M. L., McGrath, C. J., McGill, T. E., Jorgeson, J. D., and Talbot, C. A. 2007. "Geologic Setting of Mosul Dam and Its Engineering Implications." USACE, Engineering Research and Development Center. https://apps.dtic.mil/dtic/tr/fulltext/u2/a472047.pdf.

Applying Double Skin Façade with ETFE Membrane Assembly for Energy Saving and Acoustic Protection for the Building of the Czech Institute of Informatics, Robotics and Cybernetics in Prague

Petr Franta[1, 2]

1. Architects & Assoc., Ltd., Prague, Czech Republic

2. Czech Institute of Informatics, Robotics and Cybernetics—Czech Technical University, Prague, Czech Republic

Abstract: Multidisciplinary, integrated planning approach by architects, engineers, scientists and manufacturers to reduce energy consumption of buildings. The CIIRC Complex, located on the main campus of Czech Technical University in Prague consists of two buildings, newly constructed building and adaptive reuse of existing building. CIIRC—Czech Institute of Informatics, Robotics and Cybernetics is a contemporary teaching facility of new generation and use for scientific research teams. New building has ten above-ground floors, on the bottom 4 floors of laboratories, scientist modules, classrooms, above are offices, meeting rooms, teaching and research modules for professors and students. Offices of the rector are on the last two floors of the building. On the top floor is congress type auditorium, in the basement is fully automatic car park. Double skin pneumatic cushions façade. In the project are introduced series of architectural and technical features and innovations. Probably the most visible is the double skin façade facing south-transparent double layer membrane ETFE (Ethylen-TetraFluorEthylen) cushions with triple glazed modular system assembly. Acting as solar collector, recuperating of hot air on the top floors, saving up to 30% of an energy consumption.

Key words: Double skin façade as solar collector, ETFE membrane cushions as outer skin, air-recuperation from façade (top floors).

1. Introduction

Function of the building: scientist modules, computer laboratories, offices, teaching facilities.

Objective: multidisciplinary, integrated planning approach by architects, engineers, scientists and manufacturers to reduce energy consumption of buildings.

The CIIRC Complex (see Figs. 1 and 2), located on the main campus of Czech Technical University in Prague, consists of two buildings: a newly constructed building and an existing building that has been adapted for re-use.

CIIRC—Czech Institute of Informatics, Robotics and Cybernetics is a contemporary teaching facility of new generation and use for scientific research teams.

The new building consists of 10 above-ground floors: the lower four floors house laboratories, scientist modules and classrooms floors, five to nine floors above are offices, meeting rooms, teaching and research modules for professors and students. Offices of the rector of the University occupy the last two floors of the building. On the 10th floor is a congress-type auditorium, in the basement is a fully automatic car park for 190 cars (see Fig. 1).

2. Method and Materials

Double skin pneumatic cushions façade: The project introduces series of original architectural and technical features and unusual innovations. Of those probably the most advanced is a double skin façade (fifth to ninth floor) south facing with transparent double

---

Corresponding author: Petr Franta, professor, research fields: architecture and civil engineering.

Fig. 1   Double skin façade using ETFE membrane as a solar collector.

Fig. 2   The CIIRC Complex, a newly constructed building in forefront.

layer membrane ETFE (Ethylen-TetraFluor Ethylen) cushions with triple glazed modular system assembly. Welded cushions are kept under constant air pressure 300 Pa, calculations of wind load pressure and snow load impacts are taking in consideration [1]. See Figs. 3-6.
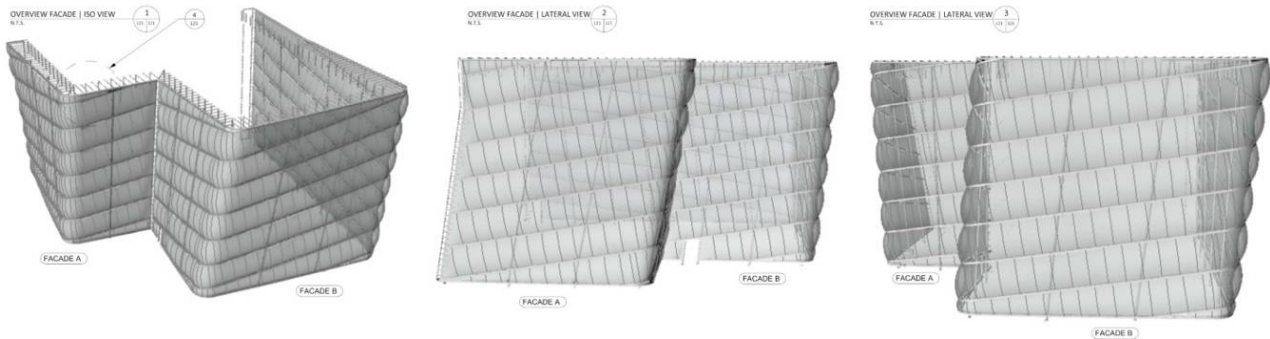

Fig. 3   ETFE pneumatic cushions façade in 3D, South and West elevations [1], showing the positions of welding seems.
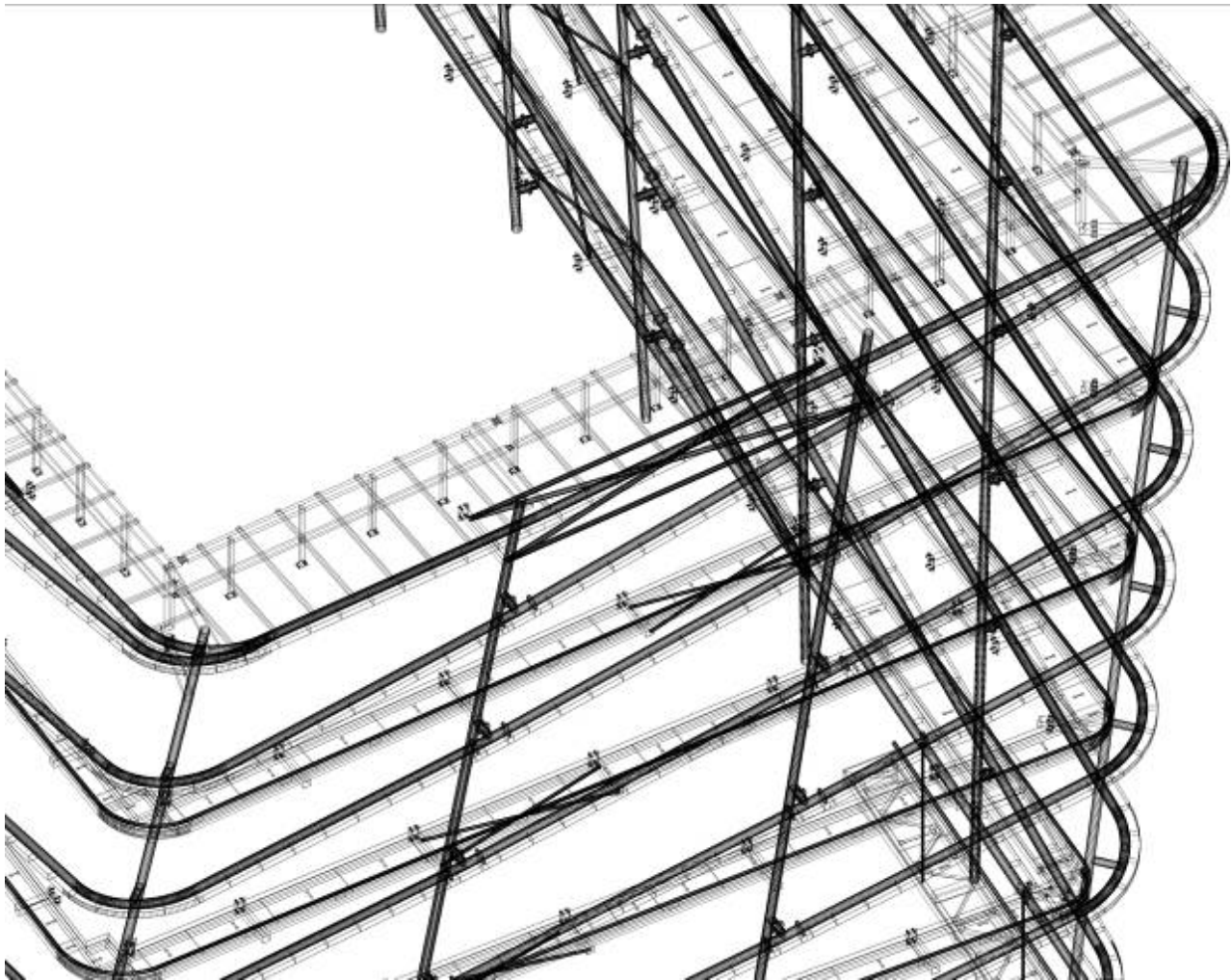

Fig. 4   Steel structure and aluminium ETFE detailing—structure engineer's 3D model [2].
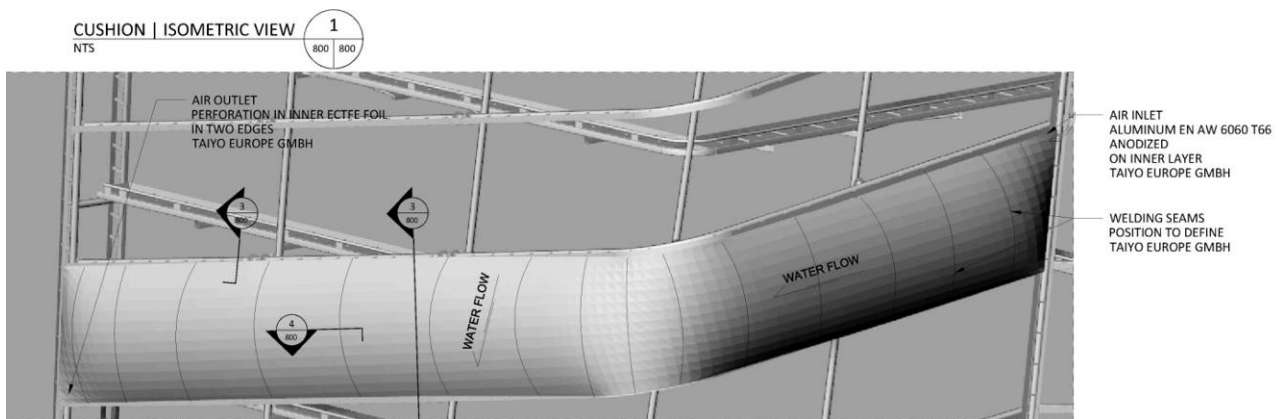
Fig. 5 Turning of the corner of diagonally placed cushion of ETFE membrane detail [1].

Fig. 6 Turning the corner—ETFE pneumatic cushions façade in 3D [1].

Transparent double layer membrane ETFE cushion with triple glazed modular system assembly acting as solar collector (see Figs. 7 and 8).

Such building envelope has high acoustic protective value (57 dB) and, at the same time is acting as a solar collector for the recuperation of hot air on the top floors, saving up to 30% of energy consumption.

Protected from the wind behind the ETFE cushions are horizontal blinds, the inner climate is controlled

by BMS system (see Fig. 7). Chilled beams are installed for heating and cooling.

Outside air is sucked into the ventilation units on each floor from two places—from the solar collector (façade between the glass facade and the facade of the ETFE facing south). From south façade for the winter and transition period and from the north façade in the summer (see Figs. 9 and 10).

Recuperation of hot air on the top floors, saves up to 30% of an energy consumption:

Fig. 7   Space between triple glazing and membrane ETFE, horizontal blinds fixed to mullions on the left. Catwalk is used for maintenance [1].
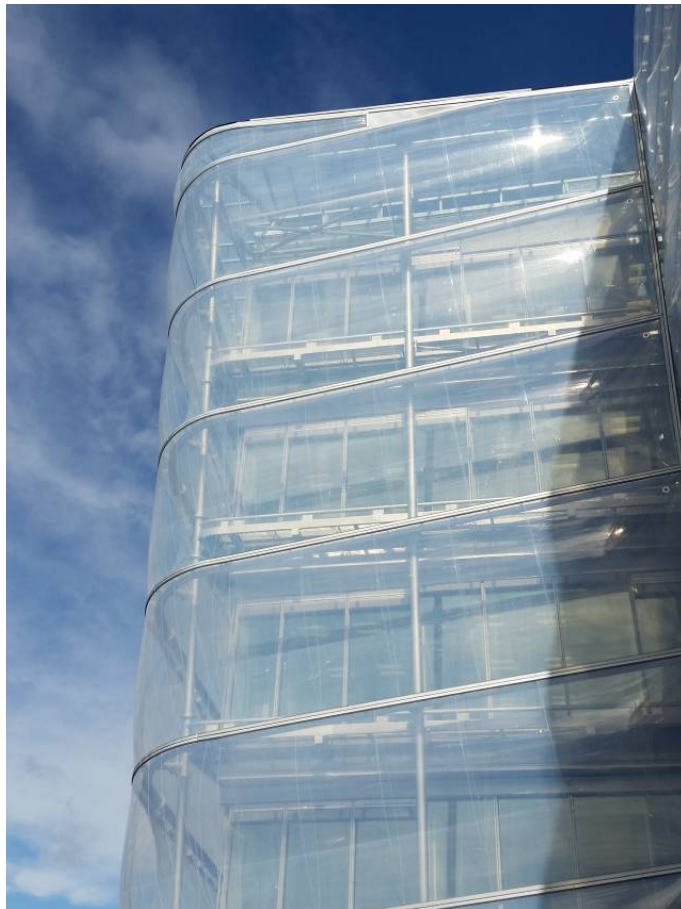

Fig. 8   Transparent membrane ETFE with triple glazing in second plane [1].
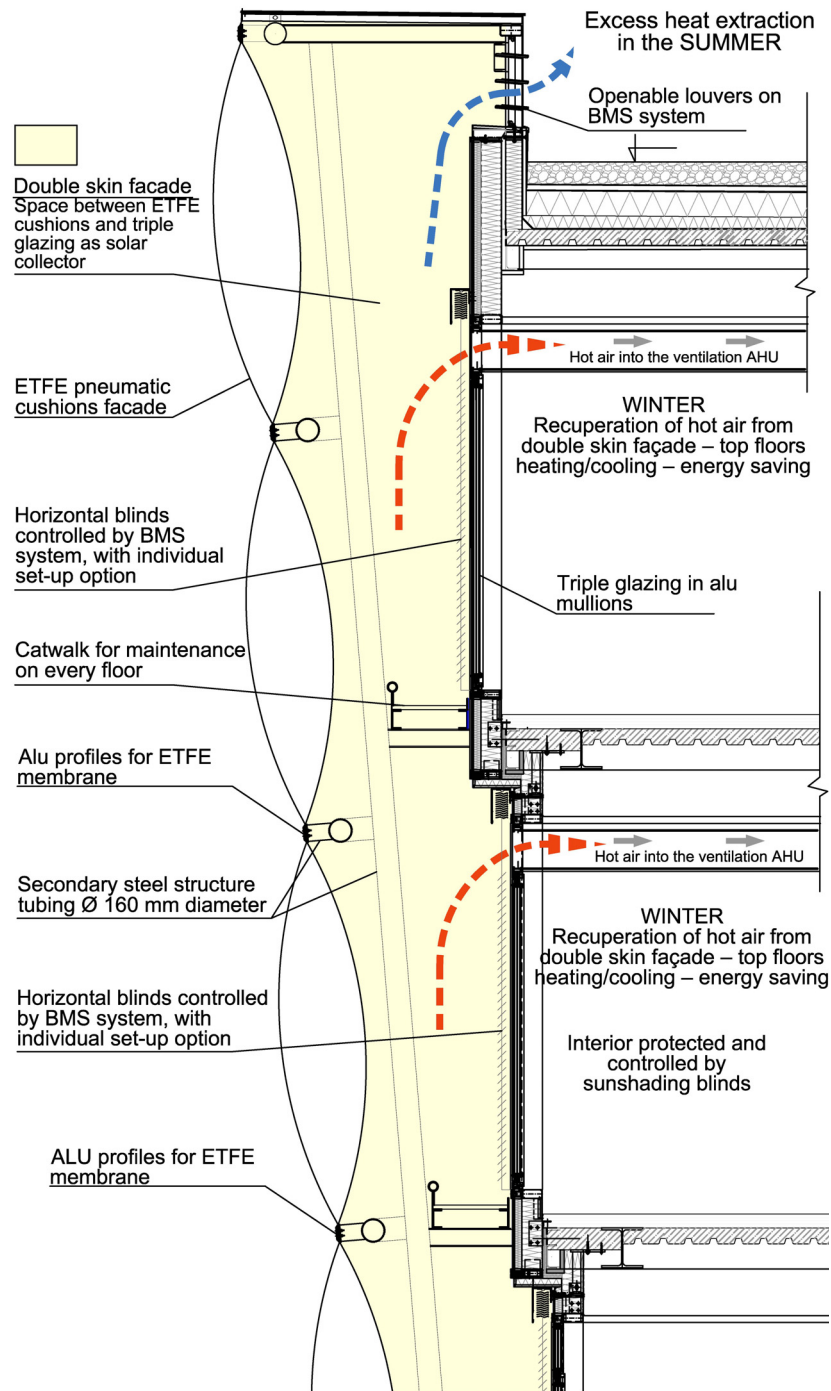
Excess heat extraction in the SUMMER

Openable louvers on BMS system

Double skin facade
Space between ETFE cushions and triple glazing as solar collector

ETFE pneumatic cushions facade

Hot air into the ventilation AHU

WINTER
Recuperation of hot air from double skin façade – top floors heating/cooling – energy saving

Horizontal blinds controlled by BMS system, with individual set-up option

Triple glazing in alu mullions

Catwalk for maintenance on every floor

Alu profiles for ETFE membrane

Secondary steel structure tubing Ø 160 mm diameter

Hot air into the ventilation AHU

WINTER
Recuperation of hot air from double skin façade – top floors heating/cooling – energy saving

Horizontal blinds controlled by BMS system, with individual set-up option

Interior protected and controlled by sunshading blinds

ALU profiles for ETFE membrane

Fig. 9   Detail of air-recuperation on the last floors [3].

Fig. 10   Schema of recuperation and air distribution to chilled beams [3].

In the laboratories, lecture halls and offices, chilled beams are installed for the distribution of air and heat control. For cooling those are using water with temperature above the temperature of dew point with the effect, that there is no condensation of air humidity on the cooling element, built in the chilled beams.

During cooling there is no condensation of air humidity, and thus no loss of latent cooling performance, otherwise consumed by condensation and without use is flowing into sewage. Proportion of latent cooling is approx. 30% of the overall performance, which represents the savings of about 30% of the power in the operation costs. By using the cooling without condensation we save cca 30% of energy, needed for production of cooling water performance. Cooling equipment also is using free cooling, where in lower temperature is water for chilled beams chilled/cooled directly on cooling towers, with no need for cooling compressors.

3. Results

Advantages of double skin façade using ETFE membrane for outer transparent skin are as follows:

(a) Weight is 1% of glass installation of outer skin;

(b) Larger width between structural members—longest double layer cushion 3 m wide × 62 m;

(c) Acoustical properties—in combination with triple glazing system (47 dB) adds 9-10 dB to 57 dB in composite calculation;

(d) HVAC (heating/cooling) values—recuperation of hot air from façade as solar collector—installation at top 2 floors—energy saving up to 30%;

(e) Self cleaning exterior of the façade—ETFE membrane with additive chemical component rejecting dirt-automatic cleaning of the façade with rain water;

(f) Protection of the automatic exterior blinds on inner triple glazed façade mullions;

(g) Aesthetics-added value—large span between structural members, etc.;

(h) ETFE membrane – 50-years lifespan of the material.

Acknowledgements

References

[1] Fouchier, A. 2016. *CVUT Prag, Paper 07 – Extrusion analysis_ind1*. Nantes, France: LEICHT, Structural engineering and specialist consulting GmbH, 2015 (13pgs.) – for TAIYO EUROPE GHMB, Munich, Germany: Shop Drawings.

[2] Beran, J. 2018. *Celkové 3D pohledy M880 – 3D Views* [Execution Drawings]. Prague, Czech Republic: EXCON.

[3] Franta, P., Farka, J., and Sekera, S. 2017. *CIIRC – Řez dvojitou fasádou s nasáváním pro rekuperaci – Section through double facade space with air recuperation scheme* [Execution Drawings]. Prague, Czech Republic: PETR FRANTA ARCHITECTS & ASSOC., Ltd..

Dynamism and Soft Robotics in the Intelligence of the New Design of Lightweight Envelopes

Consiglia Mocerino

Already contract professor in the Faculty of Architecture, Sapienza University of Rome - Miur, Rome, Italy

Abstract: The innovation of building envelopes is densely characterized, in the new design process, by new products of the building industry and intelligent robotic systems, making them efficient and dynamic in an eco-efficient environmental context and spatial flexibility. The goal is that of energy efficiency and environmental sustainability that invest above all the building production sector, pushing towards a circular economy with the use of clean energy resources and new artificial intelligence systems. The intelligence is highlighted through the optimization of the performance of new lightweight envelopes, in the technological design and the new building process, through Lean planning and Lean construction, Mass customization, with application of criteria, methods and tools. So there are innovative technological solutions, for environmental comfort and energy saving, and typological solutions with high performance level, with the use of innovative, adaptive, advanced, light materials with nanoproducts, intelligent IT systems, etc. We highlight the effectiveness of design with natural passive use of renewable energy and energy efficiency of the envelope as "skin" and relative increase in performance levels, in the interaction with the internal environment and natural dynamic flows and in the conversion of thermal and electrical energy. The methodologies are aimed at the application of digital technologies and soft robotic systems for the management and quality of services with technological and constructive solutions for dynamic interactive envelope and intelligent systems of double or triple skin, curtain walls, etc. The challenge is new design models of dynamic enclosures, on criteria and methods that guide the new rules on energy efficiency in buildings, for environmental sustainability and housing quality with the integration of soft robots.

Key words: Innovation, process, digital technologies, envelopes, soft robotic systems, sustainability.

1. Introduction

The design of buildings is changing according to the emerging needs that consider climate change with the development of digital and biocompatible technologies, while respecting the environment, focusing on quality and budget containment on sustainability and efficiency criteria.

For this reason, we aim at approaches of systemic sustainability in Architecture and related technical feasibility with the control of quality and management, of the various design choices, of a new building process with its impact on the environment, the know-how of techniques and technologies, and product innovation, and tools for evaluating the

performance characteristics of interventions.

In fact, the objectives of the new design are based, above all on the low environmental impact and on the quality of building interventions with construction efficiency, necessarily conforming with project choices and requirements, with related alternatives, also depending on the resources available to combat climate change.

So we aim at a conscious approach to the new design, with in-depth knowledge of the choices made and aimed at new construction and the built, to the sustainable urban and territorial contextualization, in which the control and maintenance of building quality are fundamental in relation to the phases of life cycle. Designers must know how to interpret the new requirements, through the innovation of the design and construction process with design industrialization, prefabrication off-site, the digitization of new

Corresponding author: Consiglia Mocerino, Arch. Ph.D., professor, research fields: technological innovation, sustainable and smart systems, energy and environmental requalification of buildings.

construction models by integrating passive systems of renewable resources into lightweight dynamic envelopes Fig. 1 [1].

They are characterized by technological systems of highly performing façades, with double or triple skin types, through an efficient design that gives dynamism and efficiency to the envelope, both for the architectural configuration, according to an aesthetic request and for the technological and constructive solutions adopted with energy efficiency and relative savings.

The methodologies are distinguished in the application of digital technologies and intelligent soft robotic systems, collaborative algorithms that enable digital transformation and make efficient systems adopted in dynamic moving and energy efficient envelopes.

They comply with European standards with new Directive 2018/844/EU updating the two previous directives 2010/31/EU and 2012/27/EU, respectively on energy performance and efficiency [2].

In these political and regulatory strategies, the construction is a determining factor for CO_2 reduction, as it accounts for around 40% of the pollution, so the types of dynamic lightweight envelopes are successfully adopted by denouncing the technological transfer, of a synthesis between science and practice, and aimed at energy efficiency.

In fact, the passive solutions that replace the efficiency of the systems, through the design with shaded areas and light, realize the interaction with the internal and external environment as a ventilation filter of natural dynamic flows, reducing the installation energy plant.

The types of reactive envelopes play a crucial role in the different urban and landscape contexts, reacting with kinetic energy to the local climate and determining the optimal internal microclimate.

This involves the advantage of reducing CO_2 through the configuration, with components and materials (glass, composite aluminum, nanomaterials, multilayer layering textiles, vertical green, PTFE-Polytetrafluoroethylene, FRP-polymer matrix fibers, EFTE-Ethylene tetrafluoro-ethylene, copper, etc.) of lightweight envelopes with moving facades, as they are equipped with digital sensors and advanced smart materials and engineered materials [3]. For this purpose there are different types including User-Control Dynamic Façade, such as the Centercity Gallery by UNStudio in Korea with Moire effect, Seasonal Green Dynamic Façade, Wind Responsive Dynamic Façade, Light Control Dynamic Façade, etc.

So lean planning and lean construction strategies are adopted in the technological design and of the new building process, with criteria of modular design and of process innovation, for the implementation of a production method with variations for techniques, technologies, equipment and/or software.
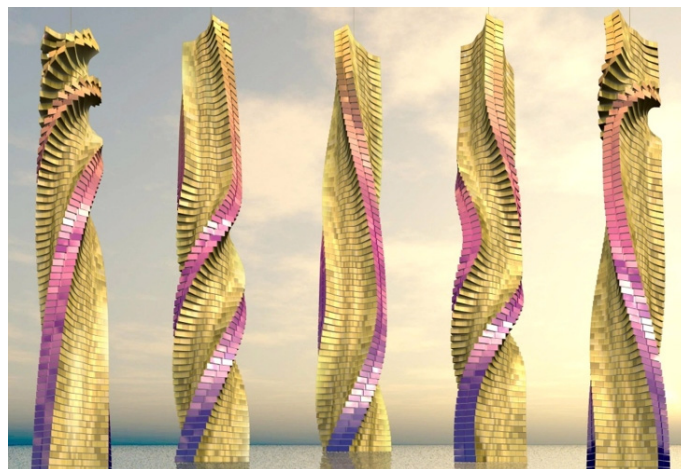

Fig. 1   Dinamic Skayscrapers-Project, by 2020. Dubai. Project with rotation of the shapes. Source: Ref. [4].

Mass customization strategies that overlap the industrial production, with the use of computerized systems, 3D printers, achieve customized results according to the needs of users for the production of complex shapes with innovative products, and representing an added value, depending on the needs flexibility in the construction sector. To this are added criteria of both radical and incremental process innovation, of a product for the improvement of technical functionalities, for components and materials, of embedded software, for ease of use or other functional features, etc.

So application of artificial intelligence robots in prefabricated or off-site constructioned and use of responsive dynamic systems, and then recourse to IT technologies, with actuator and sensor arrays in the new configurations of lightweight envelopes in a professional interoperability according to STEM (Science, Technology, Engineering and Mathematics).

2. The Dynamic Typologies

Process innovation indicates for integrated design, lean planning strategies in which both off-site building production and the use of BIM (Building Information Modeling) represent the fundamental tools to ensure efficient and effective execution in construction by signaling a revolution in AEC (Architecture, Construction and Engineering).

The new processes indicate the Lean Construction [5] that pushes to interoperability and denotes the development with the methodologies of innovation with LPS (Last Planner System), in which a team leader decides how long an activity must last on the construction site and not on the site manager.

So strategic methodologies are highlighted with the aim of new technological design, for dynamic kinetic enclosures, which is based on low environmental impact, both summer and winter comfort, and considers contextual, architectural and climatic indicators, calculating static values and transmittance indices, depending on the conductivity and thicknesses of the materials.

For this purpose, in order to design the dynamic kinetic envelopes, static and transmittance values are considered, as a function of the conductivity of the materials in self-sufficient and prefabricated building systems. Usually envelopes of the same average transmittance and the same configuration correspond to the same energy balance, even if they find disparities, between winter and summer season, in calculation models, in semi-stationary regime.

The criteria are those of new production models with awareness of the impact, of economic activity, of the environment, using fewer resources, as an index of sustainability, at a level of production and development parity using more resources.

Furthermore, they are identified the criteria of process innovation are radical, conceived as a new method or production system, such as to have no parallel in past history, which incremental process, considered as the improvement of an already existing production process, improving production efficiency and using a different combination of production steps or a technology. So tools with an off-site construction and application of intelligent construction technologies, according to the ISO 8402 and UNI 10838 standards and the new European directives on energy efficiency 2018/844/EU that update the two previous directives 2010/31/EU and 2012/27/EU, with targets for the reduction of greenhouse gases by 2050 and production of 32% of renewable energy by 2030.

The European Commission also establishes the identification of the smart indicator, by the end of 2019, as a tool capable of identifying the capacity of buildings, of improving network and operational interconnection, and finally adapting energy consumption according to the real needs of individual users. Therefore, through the control with intelligent devices of automation systems integrated by soft collaborative robots, they improve the functionality and capacity with energy saving features of buildings.

In particular, self-sustaining and prefabricated

construction systems methodologies of lightweight dynamic envelopes, which guarantee an optimal internal microclimate and reacting to summer and winter climatic excursions, maximize efficiency, guarantee environmental safety control and minimize demolitions with ecological recycling.

In this constructive typology of light prefabrication systems, we highlight the performance capacity of systems and products with durability of the same and of the components, in the eco-sustainable control of energy production and building automation, with intelligent energy solutions and incentives for companies and reduction of costs.

In fact, for the dynamic typologies some design and constructive technological solutions are adopted with actuator matrices, through responsive dynamic systems, unlike physical dynamical systems that without electrical or control devices interact passively with the external environment.

These envelopes include passive energy systems in façades, such as blackout slats for the optimization of energy performance by converting solar radiation into thermal and electrical energy, with a relative reduction in energy consumption or mobile modular systems

equipped, with sensors that react to the climate temperature and identify themselves in different forms and then restore the main form. Or installations of interactive devices capable of involving visitors through a dynamism of components with lights, interactive paintings of nanomaterials that control and reflect light, etc. From the different types of envelopes such as Insitut du Monde Arabe, Jean Nouvel in Paris to the most daring and efficient, Kolding Campus in Denmark, to the restyling of the SFMOMA (San Francisco Museum of Modern Art) realized by Snøhetta studio, with panels of a polymer fiberglass-reinforced (Fig. 2), integrated in surface by silicate crystals, and variable sunlight. This new architecture is the requalification project with integration and expansion of the MoMA Museum designed by the architect Mario Botta in 1995

As at the Hyundai Pavilion of Asif Khan Designs—The World's First Super-Black Building for the Pyeongchang 2018 Olympics, South Korea, as the pilot project of the House of Natural Resources with the adaptive solar façade, of ETH Zurich, Media-TIC Building in Barcelona with covering in EFTE material, etc. They are integrated with the User-Control Dynamic

Fig. 2   SFMOMA by Snøhetta studio. San Francisco, CA-USA. Detail of panels of a polymer fiberglass reinforced. Source: Ref. [6].

Facade typologies in which users, through electronic devices, control the operation of blinds without using reactive systems, to Light Projection Dynamic Façades that generate optical illusions of light dynamics, through the articulation of an efficient mix of design both vertically, horizontally, obliquely, etc.

This last typologie is indicated in some architectures as in the Centercity Gallery, by UNStudio in Cheonan in Korea, on which trompe d'oeuil model, a double skin glass case and aluminum profiles, simulates moire fabric effects, with monochromatic light by day and multicolored at night, distinguishing itself as an urban lighthouse. The same UNStudio realizes a dynamic BIPV envelope, for the redevelopment of a HQ Hanwha skyscraper in Seoul, a system of sustainable interaction between inside and outside. Instead with the Light Control Dynamic Façade typology, the envelopes, as in the work of J. Nouvel of the Institut du Monde Arabe in Paris, with a centralized automation system that controls the modular diaphragms in the south façade, inspired by Mashrabiya, Arabic geometry and other architectures , including the Al-Bahr Towers in Abu Dhabi, by UNStudio, are equipped with components that, through an intelligent design, constitute shading systems on the façades, sensitive to solar radiation, with the advantage of energy saving, environmental comfort and C02 reduction of up to 40%.

In particular the Mashrabiya system consists of dynamic self-regulating modules (that open and close) and sensitive to sunlight, as in the case of the Al-Bahr Towers are coated with an innovative design in PTFE (polytetrafluoroethylene) material which improves the environmental performance of the envelope by reducing solar radiation by about 20%.

In addition, they stand out the Wind Responsive Dynamic Façade, with self-regulation of the façade components dominated by the wind directions, the Adaptive dynamic facades, of many architectures such as the MAC 5-7 Offices, in Milan, by Sauerbruch &

Hutton [7] whose casing is covered with a dynamic system of solar shading in glass slats, which responds to variations in the intensity and direction of solar radiation, and controlled by a network of sensors with automated management of BEMS (building energy management systems) of the building, Homeostatic Façade System, with nanotechnologies of a double glass and an air chamber in which a dielectric elastomer is integrated, it reacts to the temperatures by self-regulating, opening and closing, and forming a shielding, which also contributes to energy saving, etc. These typologies of dynamic envelopes are integrated in the city with configurations highlighted by new construction systems and innovative technologies, which improve the built environment with the potential to connect to IoT, smart networks, facilitating the services and quality of the inhabitants.

In fact the environment is the crucial node for the design and construction of dynamic envelopes, whose skin becomes a filter between the inside and outside of buildings for the purpose of indoor environmental comfort and energy efficiency.

2.1 Efficient Stratifications and Soft Robotics Application in Envelopes

For these dynamic envelope typologies, both adopt adaptive and intelligent component and material including PCM (Phase Change Material), exploiting the natural phenomenon of the phase transition by modifying their behavior according to the climatic conditions, also robotic membranes, as chromocene materials (liquid crystals, electrochromic, photochromic, thermochromic) sensitive to external stimulations for which they change their optical characteristics, etc.

Also with the integration of intelligent systems as TMA (thermal mass activation), EC (earth coupling), DIS (dynamic insulation systems), AIF (advanced integrated facades), in particular to such components and intelligent systems of lightweight and dynamic

envelopes in architecture, they apply, in integrated design, soft robotics to increase, specially, the balance of energy requirements from renewable resources in buildings, to reduce noise in the built environment, and in making the management of technological and plant systems more secure and independent. Inspired by the shape of origami, and contributing to the greater strength of soft robots, it is experimentation, also according to Wyss Institute of Harvard University and MIT's CSAIL (Computer Science and Artificial Intelligence Laboratory), of artificial muscles (Fig. 3) or artificial actuators—Exoskeletons—with a skeleton of material metallic, like metal springs, or plastic devices, etc.

These artificial muscles, forged with water or air and then sealed by a fabric or plastic skin, through the introduction of internal emptiness, manage to move autonomously, guided by the shape and the skeleton, without human help or energy force, in natural environments and with low environmental impact.

To this end, research has advanced in multidisciplinary fields, experimenting with prototypes and innovative models for solar adaptive façades in which to combine a dynamic, interactive aesthetic model, with energy efficiency and by eliminating in the envelope, in large part, the local climatic and environmental problems, both for new buildings and for the built.

So the prototype of adaptive solar façade as part of the EU Climate-KIC Building Technology Accelerator project, at ETH Zurich, is the interface between user and environment in which energy is monitored, through the adjustment of the individual façade modules, equipped with thin-film copper solar cells (CIGS) and located south of the natural resources house (HoNR) and managed by soft robots.

They act on the principle of the compressed chamber (three chambers supplied for each actuator) chasing the solar radiation and with the unfilled chambers the expansion inhibition takes place. The hysteresis is determined by the non-linearity of the pressure in the chamber and the inclination of the module so that it becomes one of the phenomena of careful research for the energy transition.

To these types of envelopes of integrated design, additive manufacturing methods are applied to which intelligent soft robots [8] collaborate which, through some of their components, including actuators and sensors of composite material, generate movement to the modular components and on which intelligent materials are added, of energy efficiency like PV, etc.
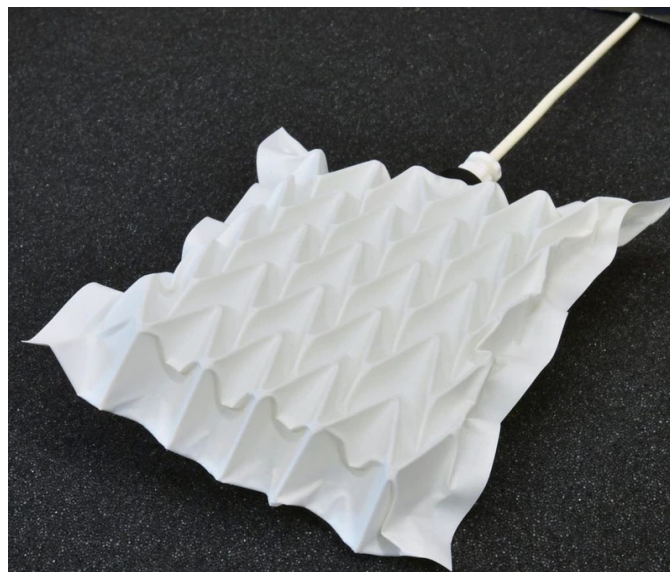

Fig. 3 Artificial muscles inspired by fluid origami. Source: Ref. [9].

In fact, the soft robots of the broad sector of artificial intelligence and learning machines, belong to one of the emerging sectors of bio robotics and are flexible, soft-structure systems that interact securely with the natural environment and the user, distinguishing themselves from rigid-structure robots.

Soft robots, usually widespread in hydrogel or silicone rubber, in which nanotechnologies are inserted, ferromagnetic, react to magnetic fields, heat or light, change shape and apply in the biomedical field, in architecture, etc. They can be lengthened, deformed and twisted taking inspiration from the forms of invertebrate plants and animal species, fluids with integrated parts, without the traditional assembly of mechanical parts of a robot and 3D printing products, such as Octobot, one of the first completely autonomous soft octopus, according to the shape of the octopus, and tested by the University of Harvard with biocompatible materials. This example of a soft robot is a pneumatic (powered by gas under pressure) type whose operation is based on a circuit which, like an electronic oscillator, controls the transformation of a small amount of hydrogen peroxide into gas, generating movement in the components of the robot.

For the power supply we used control cards, sensors, pumps, etc., instead for the modulation of the pressure inside (Fig. 4) the actuators and for movements and force, we choose feedback, finally we also resort to analytical models for the control of the state variables, when estimation difficulties arise.

According to these methods, the pressure forces, of the external objects and the internal pressure of the soft actuators, are monitored using soft sensors that are miniaturized and incorporated into the actuators themselves.

3. Case Study

Even nanotube, based coatings that cover surfaces, develop dynamism and efficiency of the envelopes, contextualizing them in the landscape or urban environment as an architectural and community focus, as well as for the Hyundai Pavilion (Fig. 6) designed by Asif Khan Designs, the world's first super black building for the Pyeongchang 2018 Olympics, in South Korea. The building with a block configuration based on criteria of Lean Construction and off-site, is developed on a 35 × 35 m square plan, 10 m high, with the space divided into five rooms that represent virtually, the water, solar energy, electrolysis, hydrogen fuel stacks and water recreation with multi-sensory installation and covered with translucent white Corian (aluminum hydroxide and acrylic resin) in interior design. The outer envelope is completely coated with a Vantablack VB×2 [12], spray
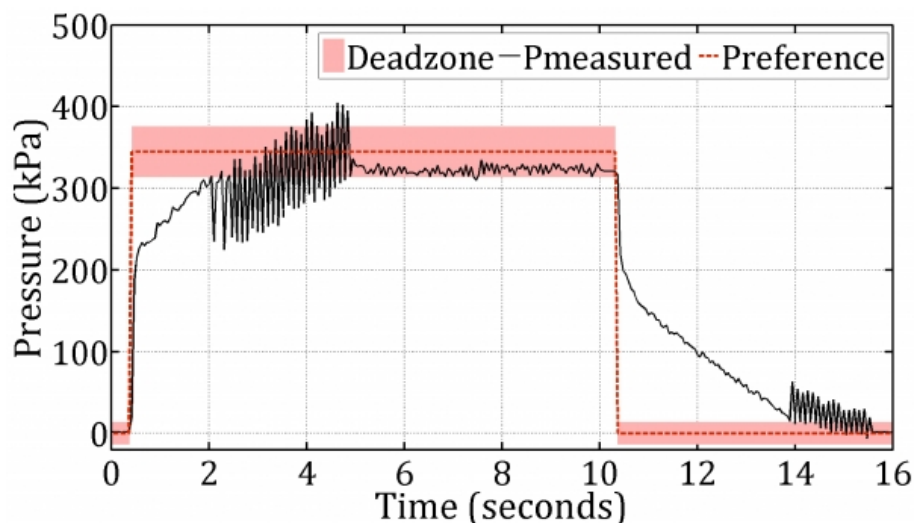

Fig. 4   Pressure graph in soft actuators through soft sensors. Soft robots-sensing and control. Source: Ref. [10].

Fig. 5   Hyundai Pavilion designed by Asif Khan at PyeongChang Winter Olympics 2018. Source: Ref. [11].

paint made by Surrey NanoSystems that absorbs 99% of sunlight creating a virtual black space void, in which thousands of bright stars spread. This nanomaterial of spray paint with THR (total hemispherical reflectance) of 1%, is adopted in architecture on different surfaces including metal, wood, polymers, ceramic, concrete, plasterboard, glass, etc. and it can also be applied to internal partitions of the building. The pigmented coating is biocompatible solvent-based dispersed in carrier solution, it is the recent version of Vantablock (a thin film of carbon nanotubes-CNT), but VBx paints do not use nanotubes.

4. Conclusions

In architecture there is an evolution of both technological and constructive systems with the increase of the fundamental know how of materials and components, with their behavior with the environment and aimed at indoor comfort and energy efficiency with the use of renewable resources.

For this purpose, scientific research and construction production, highlights in the construction sector a series of products and systems that are adopted in various building works, supported by experimentation and prototyping in which the interaction between users and dynamic enclosures integrated in particular environmental conditions occurs. The objectives of achieving sustainability with

quality of interventions, low environmental impact and energy efficiency with parametric design, for light and dynamic, adaptive envelopes are the drivers of this process innovation and digital revolution. In it the innovative materials, the nanomaterials, etc. the new construction systems with the adoption of IT, artificial intelligence soft robots, improve the performance of buildings, balancing needs and energy savings. Digital fabrication methods with intelligent systems and digital technologies that enable digital transformation, according to lean planning and lean construction and mass customization strategies, highlight in the integrated design and off-site construction of the new radical, incremental and product process, signaling a revolution in the AEC. And just in architecture the challenge is the creation of new dynamic envelopes with performance soft robots, safer, durable and sturdy that integrate with innovative technologies and materials, according to user needs, especially for the quality of the habitat with indoor comfort, energy saving and better performance of the buildings contextualized both with the built and the environment.

References

[1]   Fortmeyer, R., and Linn, C. 2014. *Kinetic Architecture: Designs for Active Envelopes.* Mulgrave, Victoria: Images Publishing.

[2]   Direttiva (UE)-EUR-Lex. 2018. Accessed July 2, 2018. https://eur-lex.europa.eu/legal-content/IT/TXT/PDF/?uri=

CELEX:32018L0844&from=en.

[3] Thomas, S., Grohens, Y., Kalarikkal, N., Oluwafemi, O. S., and Praveen K. M. 2018. *Nanotechnology-Driven Engineered Materials: New Insights.* Förlag: Apple Academic Press, CRC Press.

[4] Costruzionipallotta.it. Architect David Fisher's Dynamic Skyscraper. Accessed August 4, 2018. https://lynceans.org/tag/dynamic-skyscraper/.

[5] Seed, R. W., Beikmann, B., and Bell, C. 2018. *Transforming Design and Construction: A Framework for Change.* eBook Kindle, Lean Construction Institute.

[6] Architecture SFMOMA. 2018. Accessed March 2, 2019. https://s3-us-west-1.amazonaws.com/sfmoma-media-dev/www-media/2018/08/03004038/art-bash-facade-kam-1024x538.jpg.

[7] Mocerino, C. 2017. *Top Office Tecnologie intelligenti di riqualificazione.* Madrid: Gangemi International Publisher.

[8] Holland, D., Berndt, S., Herman, M., and Walsh, C. 2018. "Growing the Soft Robotics Community through Knowledge-Sharing Initiatives." *Soft Robotics* 5 (2): 119-21.

[9] Li, S. 2017. Wyss Institute at Harvard University Artificial muscles give soft robots superpowers. Accessed June 5, 2018. https://wyss.harvard.edu/artificial-muscles-give-soft-robots-superpowers/.

[10] Harvard Biodesign Lab. 2018. "Sensing and Control." Accessed August 3, 2018. https://biodesign.seas.harvard.edu/soft-robotics.

[11] Creative Works. Accessed March 2, 2019. https://www.creativeworks.kr/hyundaipavilion.

[12] Vantablack VBx Coatings. Accessed June 15, 2018. https://www.surreynanosystems.com/super-black-coatings/vbx-coatings.

Discharge Coefficient Measurements Using Heron's Fountain

Gevo Abcarian, Zainab Algharib, Omran Hussain, Ana Martin, Abraham Villa, Francisco Villalobos, Tadeh Zirakian and David Boyajian

Department of Civil Engineering and Construction Management, California State University, Northridge, CA 91330, USA

Abstract: Civil Engineering design students at CSUN (California State University, Northridge), aimed to demonstrate the pneumatic action of liquid water as it flows through an airtight one-way vessel system which is known as Heron's Fountain. This project explores hydraulic and pneumatics principles commonly found in environment control systems, such as the non-isothermal heating facilities located on the CSUN campus. Since this was a simply constructed version of an ancient Greek fountain, its development required the collaboration of the team to execute its simple function. The parameters involved were diameter, length, height, and density. This analysis utilizes Pascal and Bernoulli's equations to reinforce the principles of fluid mechanics. The fountain action is described based on flow rate and head loss is described by Darcy's equation. Friction loss with an angled fitting attached to the fountain head is described by Reynold's equation. The experiment observed the performances of two types of reentrant tube fittings for head loss: straight and angled. The experiment enhanced the educational experience of the research team by bringing together creative ideas from different educational and cultural backgrounds. The results of the experiment concluded with a 0.58% error for the straight fitting and 5.3% error for an angled fitting.

Key words: Heron's Fountain, hydraulic principles, air pressure, pneumatics, friction factor, engineering education.

1. Introduction

Heron's Fountain begins in antiquity with the Greek mathematician and engineer, Heron of Alexandria. He invented mechanical devices powered by air, water and steam which were used for a variety of reasons. He enjoyed using his inventions for educational purposes and taught pneumatic principles by how his devices worked. Heron's Fountain is an apparatus which responds when liquid water is added to the fountain basin and generates a water jet from the fountain head. This instrument operates using pneumatic principles and the principles of non-isothermal flow [1].

Pneumatic systems are commonly found in dams, transmission systems and power stations. Teaching the principles of hydraulics to aspiring engineers can be challenging but rewarding in the end [2]. Heron's

Corresponding author: Tadeh Zirakian, Ph.D., P.E., assistant professor, research fields: civil engineering, structural/earthquake engineering, engineering education.

Fountain is a device used to teach and demonstrate the principles of hydraulics with water and air pressure. Many scientists have dreams of perpetual motion machines that do not dissipate energy. This fountain is not continuous and therefore it is not perpetual since it only works for a certain amount of time until the velocity becomes zero [3]. The interesting device is a demonstration of hydrostatic pressure. Heron's Fountain is the first model to incorporate both automatic recharging energy and flow-triggering of the fountain [4]. Unfortunately, the fountain has several setbacks that can only be re-energized by some manual transfer of liquid which can cause liquid spillage. The team constructed the project by using plastic tanks and vinyl tubing to obtain the flow rate of the water jet and compared it to the theoretical values derived from Pascal's and Bernoulli's equations [5, 6]. Comparisons of the results were made and studied after various trials. The objective of this project is to enhance the knowledge about the principles of hydraulics in a

simple manner and to provide a better understanding of air pressure using this educational design.

The inventor, Heron of Alexandria sold his inventions to wealthy patrons who enjoyed the splendor of his mechanical inventions as centerpieces for grand occasions. Fig. 1 illustrates the original invention called "A Satyr Pouring Water from a Wine-skin into a full Washing Basin, without making the contents overflow" also known as Heron's Fountain.

2. Physical Model Details and Testing

The research team gathered reusable materials that allowed better visibility of the liquid as it runs throughout the system. The materials chosen to achieve

best results were three 1.3-gallon containers with plastic lids, vinyl tubing and adhesive shown in Table 1. It is best to construct Heron's Fountain as air-tight as possible in order to achieve best results.

2.1 Construction Procedures

Three containers were aligned in a stacked configuration. Three pieces of vinyl tubing of different diameters were cut into the appropriate lengths. Holes were drilled through the lids to pass the tubing through. With the holes aligned, the water-resistant adhesive was applied to secure the assembly and create an air-tight vessel. Silicone adhesive was also applied on the lid threads and sealed with adhesive tape. Fig. 2 illustrates the placement of the parts. As indicated in
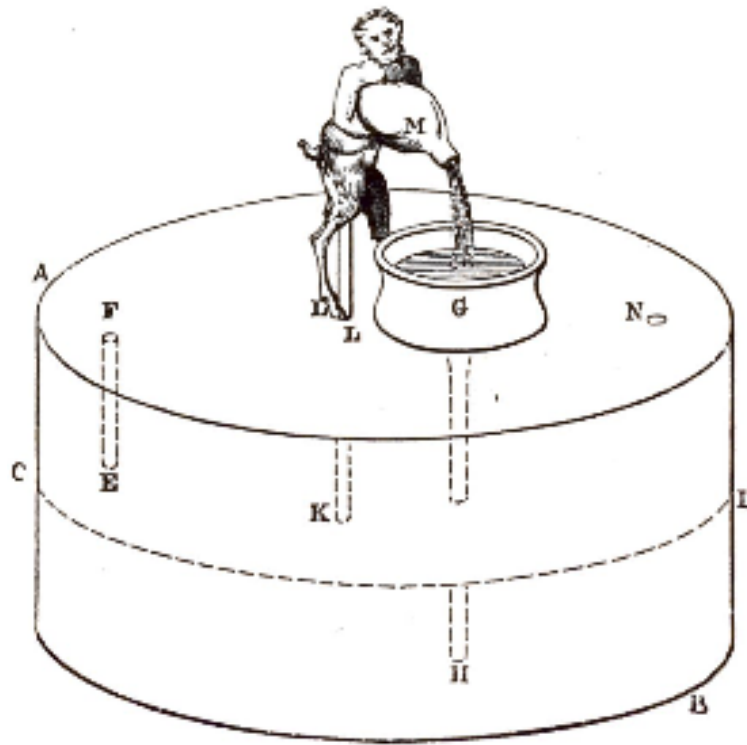

Fig. 1   Original drawing of Heron's Fountain [3].

Table 1   Orifice fittings and various vinyl tubing sizes.

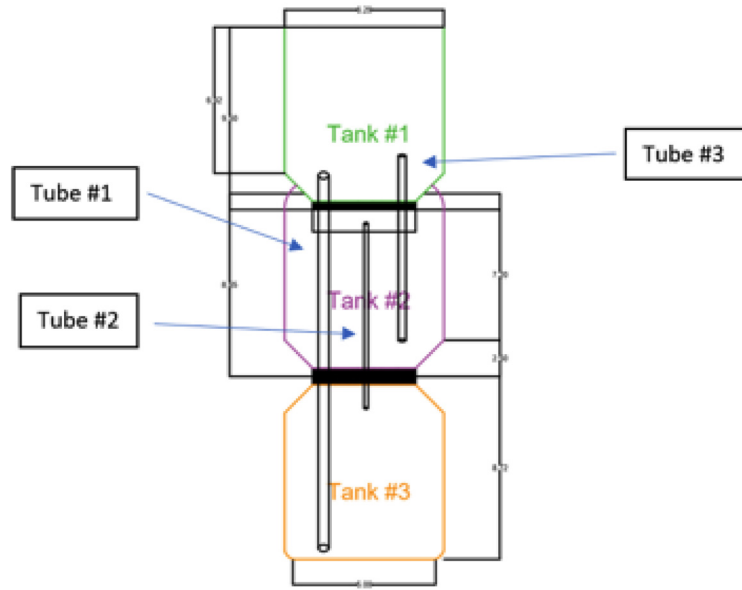| Count	Dimension	Material/Items
1	½"	Straight fitting
1	½"	90° fitting
1	¾" - 24.1" (Tube #1)	Clear vinyl tube
1	¼" - 6.50" (Tube #2)	Clear vinyl tube
1	½" - 11.8" (Tube #3)	Clear vinyl tube

Fig. 2 Project drawing of a custom-made Heron's Fountain based on original construction.

the drawing, Tank 1 is open to the atmosphere while the other tanks are closed. Tank 3 carries the stream into the basin. The fountain process was initiated by pouring water into the basin. Fig. 7, provided in the Appendix, shows the final constructed fountain.

2.2 Test Procedures

Tank 2 was filled with one gallon of warm water funneled through Tube 3. Warm water will increase internal pressure in Tank 2 as water drains into Tank 3. The rising water level inside Tank 3 generates internal air pressure, forcing air through Tube 2 into Tank 2. As Tank 2 increases in internal air pressure, this pressure forces the reserve water through Tube 3 up into the basin of Tank 1. Tube 3 is the point of the experimental control where the two fittings are attached. The hydraulic pressure is created as water enters Tank 1 and increased air pressure in Tank 3. Tank 2 creates a rising jet of water through an orifice attached to Tube 3 in Tank 1. The performance tests occur at this point with the two fittings by testing the flow rate, Q, of each orifice.

3. Theoretical Analysis

Simplicity is at the core design and construction. In

the development of the project, the use of imagination and creative thinking were used to test the performance of a variety of orifices attached to the fountain's head as shown in Fig. 3. The air pressure, P_c, in Tank 2 was determined using Eq. (1), the moment air was forced into Tank 2. Before this movement occurs the velocity of the water-level is zero. The velocity V of the water jet was determined using Bernoulli's Eq. (2) in order to calculate the flow rate using Eq. (3).

$$P_c = g(\rho_w h_w + \rho_a h_a) \tag{1}$$

where, P_c is pressure inside the middle container, g is gravitational acceleration, ρ_w is water density, h_w is height of water life, ρ_a is air density, and h_a is height of air.

$$\frac{P}{\gamma} + \frac{V^2}{2g} + Z \tag{2}$$

where, γ is specific weight of fluid, V is velocity and Z is the datum height.

$$Q = VA \tag{3}$$

where, Q is flow rate and A is cross sectional area.

4. Discussion of Results

To find the flow rate between Tank 1 and Tank 2, Bernoulli's equation was used.

$$\frac{P_2}{\gamma_w} + \frac{V_2^2}{2g_c} + Z_2 = \frac{P_0}{\gamma_w} + \frac{V_0^2}{2g_c} + Z_0 + h_f \tag{4}$$

where, head losses $= h_f =$ pipe loss + fittings losses and Pipe loss is described as:

$$h_f = f \frac{L}{D} \frac{V^2}{2g} \tag{5}$$

the expression $f \frac{L}{D} = K$ was used for the fittings. Therefore, K is classified for each type of fitting.

The general equation for head loss can be described as follows:

$$h_f = f \frac{L}{D} \frac{V^2}{2g} + K_1 \frac{V^2}{2g} + K_2 \frac{V^2}{2g} + \cdots + K_n \frac{V^2}{2g} = \left(f \frac{L}{D} + \sum_{i=1}^{n} K_i\right) \frac{V^2}{2g} \tag{6}$$

The K factors represent the friction coefficients of each fitting and are shown in Table 2 [5].

These angled fittings are attached at the threated side which is indicated as the entrance, as shown in Fig. 3.

Eq. (4) is used between Tank 1 and Tank 3 to determine pressure at Tank 3, P_3. Because the cross-sectional area of Tank 1 is equal to the cross-sectional area of Tank 3, $V_0 = V_3$ therefore V_0 and V_3 cancel and create the following expression $P_0 = 0$.

$$P_3 = (Z_0 - Z_3)\gamma_w \tag{7}$$

Eq. (4) was applied between Tank 3 and Tank 2 where $V_2 = V_3$, therefore V_2 and V_3 cancel. This yields the following equation to solve for P_2:

$$P_3 - P_2 = (Z_2 - Z_3)\gamma_w \tag{8}$$

Pressure at each point is determined by applying Eq. (4) with the head losses to find the velocities in the pipes.

Eqs. (4) and (5) were applied to Tank 1 and Tank 2 to solve for V_{P3}. The theoretical flow rate of the straight fitting is $Q_3 = A_{P3} * V_{P3} = 0.0067 \left[\frac{\text{ft}^3}{\text{sec}}\right]$. The experimental average flow rate concluded was $Q_{exp} = 0.00705$ [ft^3/sec]. The expression used to determine this percentage is:

$$\% \ error = \frac{Q_{exp} - Q_3}{Q_3} * 100 \tag{9}$$

This yields the percent error to be 5.3%.

The theoretical flow rate of the angle fitting is $Q_3 = A_{P3} * V_{P3} = 0.0058 \left[\frac{\text{ft}^3}{\text{sec}}\right]$. The experimental average flow rate concluded was $Q_{exp} = 0.00566$ [ft^3/sec]. yielding to a percent error of 0.58%. Sample calculations of friction factor (f) are provided in the Appendix.

Table 2   Friction constant values of each reentrant fitting.

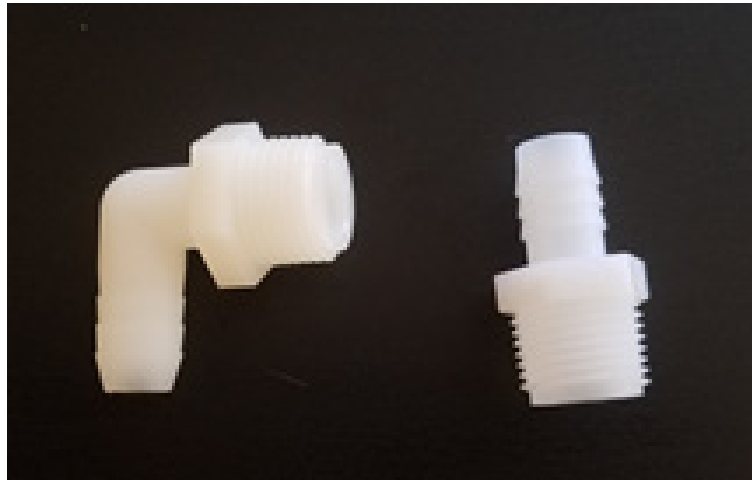| Experiment	K_1 Entrance	K_2 Elbow	K_3 Exit
#1 Straight fitting	0.78	-	1
#2 90° fitting	0.78	30	1

Fig. 3   Fittings: ½" - 90° (elbow) and ½" - 180° (straight).

The experimental research indicates the flow rates of angled and straight fittings at three separate trials. As shown in Figs. 4 and 5, the correlation among these flow rates per each trial for angled and straight fittings is 99% based on the R^2 values. Due to a lower friction factor in the straight fitting attachment, the flow rate through the system was more efficient.

The theoretical velocity for the straight fitting was 4.91 [ft/s] while the angled fitting was 4.23 [ft/s]. The experimental velocity for the straight fitting was 5.2 [ft/s] while the angled fitting was 4.29 [ft/s]. The velocity value in the angled fitting is less than the velocity in the straight fitting for both the experimental and the theoretical due to the head loss in the angled fitting. The research team came to the conclusion that the percentage error for the straight fitting and the angle fitting were due to the size of the tubes, since Tubes 2 and 3 are smaller in diameter compared to Tube 1. Minor leakage of air pressure tends to give such percentage of errors.
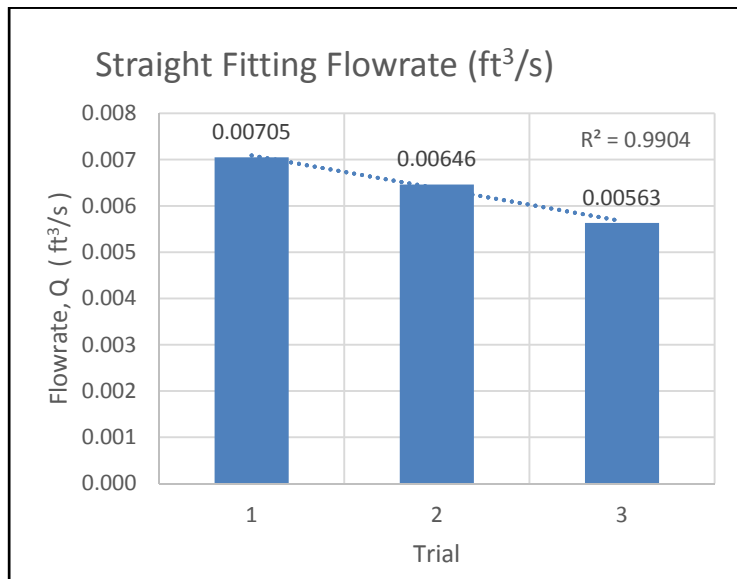

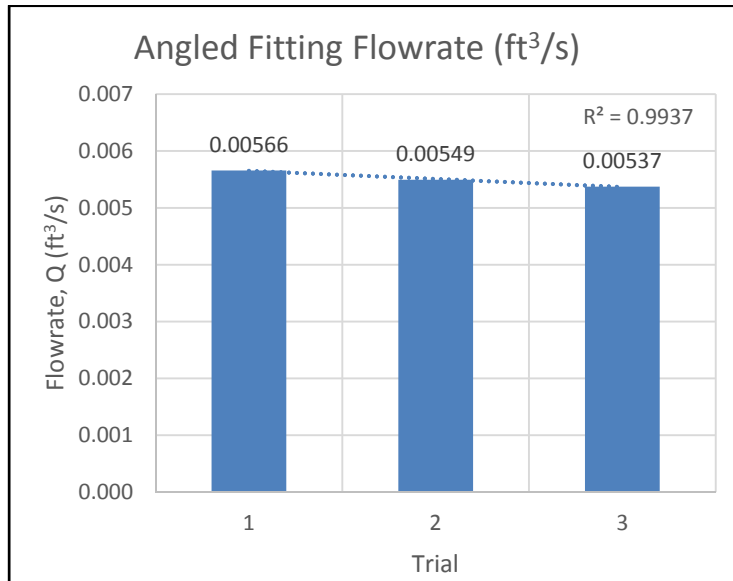Fig. 4   Straight fitting flow rate per trial.

Fig. 5   Angled fitting flow rate per trial.

Fig. 6   Group member Francisco Villalobos demonstrates Hero's fountain at student youth STEM program.

5. Educational Objectives

Each member in the research team was able to understand basic hydraulic principles that this device teaches. With students having different backgrounds and different levels of knowledge about the subject, it was necessary to discuss and conduct research about the topic with one another throughout meetings. Learning about hydraulics in this simple manner will provide a better comprehension in future related classes and professional practice. Furthermore, the members were able to gain theoretical knowledge on how to apply Bernoulli's equation to a hydraulic mechanism in which enhances members' understanding about the analysis and properties of fluids.

Every member in the research team comes from a minority background, including women in engineering. Through teamwork and creativity, the students were able to bring this effort to light, despite different cultural backgrounds. This model could be used to cast attention on science and engineering to young high school students, as it can be explored by them physically. In addition, the members of the research team can serve as role models to younger minority students. This effort was demonstrated to the student youth at a Los Angeles STEM program as seen in Fig. 6, which carries on the tradition of hands on learning and teamwork.

During this demonstration, the children were able to have a hands-on learning experience by capitalizing on the fountains size.

This presentation included a brief presentation with slides of pictures, graphs and results. This collaborative effort utilized simple techniques and methods to conduct the experiment and produce results. The design and construction used a creative approach to test the flow rates of two types of orifice reentrant fittings attached to the fountain's head. The collaborative nature of the project brought purpose and meaning to the project while enriching the participation in the research of this ancient invention that was modeled for teaching purposes. Heron's invention was used as a basis to test the performance of the attached fittings.

6. Conclusion

In this educational research, Heron's Fountain was designed, constructed, tested, and theoretically analyzed. This project was conducted to find the flow rate of two different orifice fittings, including a straight orifice and an angled orifice. Many principles have been used in this project such as, the flow rate equation and the Bernoulli's, Darcy's, and Reynold's equations. Therefore, this research effort has enhanced the usage of such equations and engineering applications. Some challenges the research team experienced included, where to begin the construction, finding the pressure of the Tanks, and preventing leakage. The team was led by

women in engineering and with their innovative ideas, the goal was achieved after discussing different approaches that could be applied to this project. Through intense research, the team was able to find a solution to finalize the Heron's Fountain project.

Acknowledgments

References

[1] Kezerashvili, R., and Sapozhnikov, A. 2003. "Magic Fountain." Arxiv ID: physics/0310039. ArXiv.org, Cornell University.

[2] Georgescu, A.-M., Georgescu, S.-C., and Stroia, L. 2014. "Heron's Fontaine Demonstrator. Revista Română de Inginerie Civilă." *Romanian Journal for Civil Engineering* 5: 87-94.

[3] Greenwood, J., and Woodcroft, B. 1971. "The Pneumatics of Hero of Alexandria" introduced by Marie Boas Hall.

[4] Ong, P. P. 1992. "Hero's Fountain: Reversible Model. (Apparatus for Demonstrating Hydrostatics)." *The Physics Teacher* 30 (7): 436.

[5] Lindeburg, M. 2018. *PE Civil Reference Manual* (16th ed.). Belmont, California: Professional Publications, Inc.

[6] Gerhart, P. M., Gerhart, A. L., and Hochstein, J. I. 2016. *Munson, Young, and Okiishi's Fundamentals of Fluid Mechanics* (8th ed.) New Jersey: Wiley.

Appendix

Fig. 7   Final construction of Heron's Fountain. Based on the schematic diagram the fountain was constructed and tested until there was no leakage.

In addition, sample calculations for determination of the friction factor are also provided in the following. Two methods were used to solve for the friction factor for A. the straight fitting and B. the angle fitting.

A. Solving for the friction factor as a function of Reynold's Number

Considering $\epsilon = 0.0006\ in$ for a plastic pipe, we can get:

$$\frac{\epsilon}{D} = 0.0001$$

An initial approximation of Reynold's can be obtained by using the experimental velocity $V = 5.2\frac{ft}{sec}$

$$\nu = 0.0000092\ \frac{ft^2}{sec} @ 80^0 F$$

$$Re = \frac{DV}{\nu} = 23550 > 4000$$

Therefore, the flow is turbulent:

From the Moody Diagram with $\frac{\epsilon}{D} = 0.0001$ and $Re = 19300$, therefore is **f = 0.0278**

B. Solving for the friction factor using the experimental velocity

As a first approximation $V = 4.26\frac{ft}{sec}$, so

$$Re = \frac{DV}{\nu} = 23550 > 4000$$

Therefore, the flow is turbulent:

From the Moody Diagram with $\frac{\epsilon}{D} = 0.0001$ and $Re = 19300$, therefore is f = **0.028**.

Note that only in laminar flows does the following apply (Re < 2100): $f = \frac{64}{Re}$.

A Civil Engineering Senior Design Research Effort to Ascertain Discharge Coefficients of Different Orifice Geometries

Abdalla Alajmi, Sayed Sayed Ali, Mohammad Alkhudhari, Jumana Alqaffas, Zack Carrasco, Jocelyn Payan, Martin Pasamba, Tadeh Zirakian, and David Boyajian

Department of Civil Engineering and Construction Management, California State University, Northridge, Northridge CA 91330, USA

Abstract: The present researched topic was conceived from a senior design course for Civil Engineering students at CSUN (California State University), Northridge. In this work, experimental trials were performed and compared to establish theoretical values of the discharge coefficient. The discharge coefficient is a dimensionless number used to characterize the flow and pressure loss behavior of nozzles and orifices in fluid systems. A group of low-income undergraduate students with diverse backgrounds designed multiple 3D printed orifices where each 3D printed orifice had a specific shape. Utilizing the methods of technical problem solving, the undergraduates found experimental discharge coefficient values for the following orifices: borda, short-tubed, and sharp-edged. Implementing ethics of engineering practice and utilizing university resources, this study is a representation of the collaborative work of minorities and females that want to expand their knowledge within their respective discipline of Civil Engineering.

Key words: Education, orifice, 3D-printing, theory, test.

1. Introduction

To determine the discharge coefficient of the different 3D printed orifices, multiple trials for each orifice were conducted. The design and calibration are very satisfactory for use as primary standards [1]. Knowing the vessel's diameter, the height of the water from the designated datum, and orifice dimensions, the discharge coefficient C_d was calculated. The three orifices that were used during tests are borda, short-tubed, and sharp-edge with theoretical discharge coefficients of 0.61, 0.62, and 0.51 respectively. Calculated experimental data were compared and analyzed to theoretical data.

Orifices are defined as openings, which are placed well below the upstream water level, and are commonly used for water flow [2]. Time of drainage is one of the major factors when calculating the discharge coefficient. The time of drainage is dependent on the geometry of the orifice opening. Based on the tank dimensions, and correct C_d, the drainage time can be calculated. Ref. [3] demonstrated that a 0.61 C_d should be used for an actual, sharp edged orifice.

In this research, comparison is made between experimental results and theoretical predictions. One of the purposes in this effort was to educate students with diverse backgrounds about how mechanisms such as this are built and can yield nearly similar results to theoretical published values. There were slight discrepancies between experimental and theoretical data which were due to the principle fabrication errors of the orifice, experimental setup of the orifice which led to minor leaking issues. The orifices used in experimentation were 3D printed.

Corresponding author: Tadeh Zirakian, assistant professor, research fields: structural and earthquake engineering. E-mail: tadeh.zirakian@csun.edu.

2. Orifice Geometry

3 PLA (Polylactic acid) 3D printed circular orifices of ½ in. diameter were used in the experiment (Figs. 1-3). The circular orifices were 3D printed to replicate the theoretical orifice shapes borda, short-tubed and sharp-edged to investigate whether the calculated experimental discharge coefficient was similar to the theoretical constant. In this experiment, the discharge coefficient C_d was calculated by recording the drainage time of water from a specific height to the specific datum. The three orifices were designed to have equal areas to limit the number of variables and experimental errors. The purpose of this experiment was to calculate the discharge coefficient, the coefficient responsible for mass flow rate ratio in respect to nozzle discharge. To compare the theoretical value, the research students replicated illustrations shown in the senior design course based on a figure "Discharge from a Tank" [4].

For Figs. 1-3, each was hand calculated to have the same cross sectional areas. Figs. 1-3, demonstrate all orifices to have an exterior diameter of 2 inches. The orifices were then modeled on AutoCAD Inventor, a 3D modeling software used for parametric modeling.
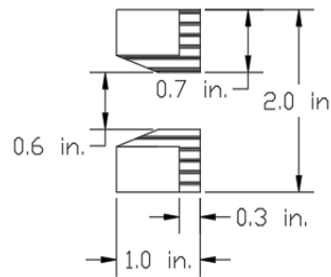

Fig. 1   Borda.

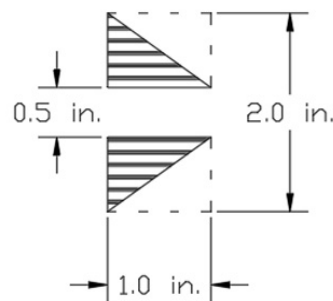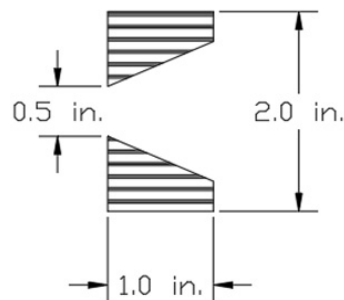**Fig. 2   Short-tubed.**

Fig. 3   Sharp-edged.

3. Testing Details

Two containers were positioned with a significant elevation to allow uninterrupted water flow between the water container with the orifice and the collecting container. The orifice was placed within a male adapter surrounded by a washer to prevent any leakage. The adapter was placed in the container to be tested (Fig. 4). The experiment was performed five times per orifice. Student researchers were assigned specific roles consisting of a spotter and three timekeepers. The spotter was in charge of releasing the water cork to allow the water to flow, therefore announcing the start and end of the experiment. The three timekeepers were assigned to time the experiment starting with the release of the cork and stopping when the spotter announces that the water has reached the orifice. The reason behind having multiple time keepers was to reduce human error by taking the average of the three recorded times to represent a single time value.

4. Discussion of Results

The equation used to perform the calculations was utilized using resources found in Ref. [4]. The discharge coefficient of the orifice is calculated by the following equation

$$C_d = \frac{2A_t\left(\sqrt{z_1 - z_2}\right)}{tA_0\sqrt{2g}} \tag{1}$$

In Eq. (1) the area of the tank A_t was kept constant for each trial, using the same apparatus to conduct the experiment. The value for the A_t, was 103.81 (in^2). The distance between the height of the water, Z_1 to the center of the orifice, Z_2, was 9 (in). The datum was set to be the center of the orifice, Z_2. The areas of each orifice, A_0, were designed to be of equal value of 0.283 (in^2). The results had an error of 29.78% for borda, 0.23% for short-tubed, and 9.93% for sharp-edged as shown in Table 1.

The varying degrees of discrepancies in this study can be attributed to two major components: fabrication

Fig. 4   Experimental setup.

Table 1 Comparison of test and theoretical discharge coefficient.

	Theoretical	Experimental	Error (%)
Borda	0.51	0.726	29.78
Short-tubed	0.61	0.611	0.23
Sharp-edged	0.62	0.688	9.93

and modeling. The student researchers designed the orifices with similar dimensions to attempt to replicate theoretical values. However, after the orifices were fabricated using 3D printers, there were slight dimensional discrepancies, borda in particular with a length dimension of 2 inches as opposed to 1 inch, which would account for the largest experimental error. It was found that the different printing temperatures of the white PLA yielded different ultimate tensile strength and percent crystallinity results as well [5]. The modeling of the experimental apparatus also contributed to theoretical discharge coefficient discrepancies.

5. Educational Objectives

An important aspect of this experiment was to understand the basic fundamental concepts of hydraulic design pertaining to Civil Engineering using research techniques. Knowledge about the orifice coefficients and discharges through circular and rectangular orifice is very important when determining its usage based on the low or high discharges as well as high or low orifice coefficients [6]. As students with different learning capabilities, this experiment integrates engineering and research as a tool to engage students in the active learning process. Another important facet of this experiment was the knowledge gained through the application of theoretical information to real world practice, paramount to developing skills that may be applied to students' respective discipline of engineering. Through these research techniques the development of mathematic principles, as well as discerning experimental, theoretical and numerical based information are reinforced. These educational pedagogies set a precedent for future success in engineering courses and educational practice.

6. Conclusion

The student researchers were required to learn a brief introduction into fluids mechanics in order to progress throughout the experiment. Results varied on error percentage when comparing experimental and theoretical values. Head loss due to friction was ignored due to length not being a considerable factor for any pressure loss calculations. Variables such as areas, height and time were crucial when calculating the discharge coefficient. The student team of researches benefited greatly by visualizing and analyzing the behavior of liquids in motion. All the knowledge gained from the water resources module, a section from the senior design course, guided the students to understand the concept and purpose of the experiment performed. Throughout the course of this experiment, the team of researches faced many obstacles such as: leakage, scheduling, and lack of materials and tools. The success of the experiment was established on team performance, assembling of ideas, and inspiration.

Acknowledgments

References

[1]   Bean, H. S., Buckingham, E., and Murphy, P. S. 1929. "Discharge Coefficients of Square-edged Orifices for Measuring the Flow of Air." *Bureau of Standards Journal of Research* 2 (3): 561.

[2]   Hussain, A., Ahmad, Z., and Ojha, C. S. P. 2016. "Flow through Lateral Circular Orifice under Free and Submerged Flow Conditions." *Flow Measurement and Instrumentation* 52: 57-66.

[3]   Joye, D. D., and Barrett, B. C. 2008. "The Tank Drainage Problem Revisited: Do These Equations Actually Work?" *The Canadian Journal of Chemical Engineering* 81 (5): 1052-7.

[4]   Lindeburg, M. R. 2018. *PE Civil Reference Manual* (16th ed.). Professional Publications, INC.

[5]   Wittbrodt, B., and Pearce, J. 2015. "The Effects of PLA Color on Material Properties of 3-D Printed Components. Additive Manufacturing." *Additive Manufacturing* 8: 2-3.

[6]   Nicholas, A. M., and Bobai, S. B. 2018. "Determination of Orifice Coefficients for Flow through Circular and Rectangular Orifices." *Abubakar Tafawa Balewa University (ATBU), Journal of Science, Technology & Education (JOSTE)* 6 (8): 188-97.

Analysis of a Hydraulic Pipe System with Major and Minor Pressure Losses

Mohammad Alesmaeel, Ali Alfarsi, Safaa Almusa, Emilio Diaz, Souren Grigoryan, Joao Queda, Tadeh Zirakian and David Boyajian

Department of Civil Engineering and Construction Management, California State University, Northridge, CA 91330, USA

Abstract: Bernoulli's principle states that an increase in the speed of a fluid is directly related to the decrease in the fluid's potential energy. Many engineers refer to Bernoulli's equations to calculate the pressure of a system. The objective of this undergraduate research endeavor is to illustrate the accuracy of his theory and apply it to one of the most common fluid systems in residential homes, a pump pipe system. The research team consisted of a diverse body of undergraduate students with different educational and cultural backgrounds. Completing this objective further improved every member's problem solving, communication skills, self-confidence, ability to rationalize and transcribe physical phenomena as well visually express them to rest of the engineering community. The findings of this research showed a relationship between various parameters such as, pipe length, pipe roughness, diameter, and specific gravity of the liquid.

Key words: Bernoulli's equation, pipe flow, hydraulics, educational model, engineering creativity.

1. Introduction

An engineer is only as good as their ability to transcribe data through experimentation and come up with an accurate relationship of the parameters in question. This ability can only be developed through repeated exposure to diverse challenges where one must use fundamental engineering techniques and logic to express real world problems in mathematical models. After a model is accurately represented, basic arithmetic should suffice in extracting the information needed. This ability to visualize the model of the problem is what makes experience in the field of engineering so desired. The goal of this endeavor is to further heighten the creativity and understanding of conceptualization to engineering undergraduate students. When Civil Engineers are exposed to any project where fluids are concerned on of the most important parameters is pressure. The criticality for engineers to understand and calculate the pressure

values of a hydraulic system cannot be overstated. With the help of Bernoulli's equation, a theoretical model of two different points in a control volume can be related through pressure and velocity [1]. To accurately create relationships between various fluid pressure parameter, tables and charts of previous engineering lab tests were collected, including pipe roughness and pipe angle coefficients [2]. This research study explored real life problems by comparing theoretical and experimental values obtained using a physical model, as well as the use of a firsthand experimentation of Bernoulli's concepts in his *Hydrodynamica*. The objective of this research is to better explore the relationship between initial pressure and its loss within the system, the two types of loss (minor and major), and the volumetric flow rate throughout the whole system [3]. Pressure loss in a hydraulic pipe system can be further classified into minor and major losses with each being a function of different variables. Minor loss is a function of the deviations from a straight pipe flow, meaning all the turns the pipe makes using various connections. While major loss is a function of the dimensions of a certain

---

Corresponding author: Tadeh Zirakian, Ph.D., P.E., assistant professor, research fields: civil engineering, engineering education.

pipe along with the velocity of the liquid passing through it.

2. Theories and Concepts

Antoine Laviosar first stated the law of conservation of mass, which states that for any system closed to all transfers of matter and energy, the mass of the system must remain constant over time. As a system's mass cannot change, so quantity cannot be added nor removed [4]. His famous work was later used to derive a multitude of equations including Eq. (1), the continuity equation, which holds true for steady state isentropic flows such as the one evaluated.

$$Q_1 = Q_2 = \rho_1 V_1 A_1 = \rho_2 V_2 A_2 \qquad (1)$$

In Eq. (1), Q = volumetric flowrate (ft^3/s), ρ = density of the fluid (slug/ft^3), V = average velocity of fluid (ft/s), and A = cross sectional area (ft^2). Bernoulli's equation creates a simplistic model by grouping certain properties together, to create different heads of pressure that are all converted into units of height as seen in Eq. (2) [5].

$$z_1 + \frac{P_1}{\rho g} + \frac{V_1^2}{2g} + h_p = z_2 + \frac{P_2}{\rho g} + \frac{V_2^2}{2g} + h_L \qquad (2)$$

In Eq. (2), z = height of the fluid relative to a constant reference point (ft), P = pressure of fluid (lbf/ft^2), g = acceleration due to gravity (ft/s^2), h_p = pressure head of pump (ft), and h_L = the total pressure head loss (ft). The various pressure heads were identified as gravity, static, velocity, and pump respectively. Each pressure head contributes to the total possible pressure in the system, which according to Bernoulli, should be equal on both sides of an incompressible and isentropic flow (adiabatic and reversible process). His initial equation has expanded to both pumps and friction losses in a closed system. The mathematical representation of both major pressure loss and minor pressure loss can be seen in Eq. (3) and Eq. (4), respectively.

$$h_{L-major} = f \frac{(L)(V^2)}{2(g)(D)} \qquad (3)$$

$$h_{L-minor} = \Sigma K_f \frac{V^2}{2g} \qquad (4)$$

In Eqs. (3) and (4), f = Darcy's friction factor, L = length (ft), V = average velocity of fluid (ft/s), g = acceleration due to gravity (ft/s^2), D = diameter of the pipe (ft), ΣK_f = loss coefficient for pipe components. With all the variables known for minor loss, the Darcy's friction factor was the key missing element to complete the pressure loss equations. Darcy's friction factor is a factor that is dependent on what type of flow is present in the system as there are three different types of flow which behave differently. Laminar flow which is generally seen when dealing with: small pipes, relatively low velocities, is characterized when the innermost parts flow the fastest and the cylinder touching the pipe is not moving at all. Turbulent flow however is generally found in high flow rate systems with large pipes and is unpredictable due to its high velocity. In between both type of flows there is the transitional flow which is a mixture of laminar and turbulent flow. With turbulence in the center of the pipe, and laminar near the edges, each of these flows behaves in different manners in terms of frictional energy loss while flowing and has different equations that predict their behavior. To differentiate between the flows Reynolds number, a unitless parameter is used to identify the flow's behavior. This is calculated using Eq. (5).

$$Re = \frac{\rho V L}{\mu} \qquad (5)$$

where ρ = density of the fluid (slug/ft^3), V = average velocity of fluid (ft/s), L = length (ft), and μ = dynamic viscosity of the fluid (lbf.s/ft^2).

With Reynolds number known, the appropriate equation can be applied to calculate f, Darcy's friction factor, which can be later used to calculate the major pressure loss. A flow is considered laminar if the Reynolds number is below 2,000, turbulent flow is the term given to flows with a Reynolds number greater than 4,000, and transitional flow is for flows in between laminar and turbulent. The correct equation can be evaluated by using Eqs. (6)-(8).

$$\text{Laminar Flow: } f = \frac{64}{Re} \qquad (6)$$

Transitional Flow: $f = \dfrac{1.63}{ln^2[\frac{6.9}{Re}+(\frac{\epsilon}{3.7D})^{1.11}]}$ (7)

Turbulent Flow: $\dfrac{1}{\sqrt{f}} = -1.8\log[\frac{6.9}{Re} + (\frac{\frac{\epsilon}{D}}{3.7})^{1.11}]$ (8)

In Eqs. (7) and (8), Re = Reynolds number, D = diameter of the pipe (ft), and ϵ = relative roughness of pipe. With the correct equation now used and the appropriate friction factor known, Eq. (3) can be used to sum up both pressure losses, and the accumulation to the total loss in the system, h_L, which is expressed in Eq. (5). With the sum of the losses calculated using Eq. (9), and Bernoulli's equation now complete for five different pump pressures, various relationships between each type of pressure losses, volumetric flow rates, and velocity can be made to make sense of the flow.

$$h_L = h_{L-minor} + h_{L-major} \qquad (9)$$

By applying the law of conservation of energy to a fluid system, the exit velocity of the flow was able to be calculated using Eq. (1), which assumes that if the area of the pipe and the density of the liquid are constant, then the velocity of the inlet and outlet should also remain constant if friction pressure loss were to be ignored. With the velocity known for the same system with both a presence of loss (experimental) and an absence of loss (theoretical), the loss from the system due to pressure losses was calculable. Minor loss consists of the pressure difference due to entrances, exits, and different types of connection that deviate the direction of the flow from its customary direction. Where major losses sum up the pressure difference due to the friction coefficient of the material of the pipe, while also considering the dimension of the pipe, and velocity of the flow [6]. However, to calculate the major loss in a system an experimental friction factor, f, is needed which is a function of the Reynolds number of the flow. The Reynolds number, pipe coefficient and diameter of the pipe govern the friction factor and equation used. This study deals with a relatively low pipe roughness and low velocity, which translates to a

friction coefficient of 0.008 due to its laminar flow which can be found on the *Moody Chart*. This research provides a simple yet practical approach to understand how a hydraulic system works, which helps engineers design for required pump pressure and efficiency of any hydraulic system.

3. Details of Physical Model

To construct the physical model representation of the team's hydraulic system some specific materials were required. The system required five 10' ½" diameter PVC pipes, five 90°-½" and three 45°-½" PVC elbows for connections. A Kedsum 550 GPH electric submersible pump was used to pressurize the system. Two 5-gallon buckets with volumetric lines to record the volume of water going in and out of the system and all-purpose cement glue to assist with neutralization of any pressure losses to mitigate error in the experiment.

To create a system with significant minor and major pressure loss, a large system of pipes and connections had to be constructed, which was computer designed using both AutoCAD and SOLIDWORKS programs. The 5-gallon bucket was first filled above the halfway mark to have enough water for the system. The various pipes were connected to resemble the drawing on Fig. 1. While an overall plan view of the designed system is shown on Fig. 2, and the actual built model is shown in Fig. 3. To secure the piping system, an adhesive was also applied on the inner and outer layers of the connection, to make sure there is no pressure loss that is not accounted for. The pump was placed in the 5-gallon bucket and held down using the legs found on the bottom of the pump, while the other empty bucket was placed at the outlet of the system to record the volume of water coming out of the system. The pump was then turned on to pressurize the system, while also being used to check for any leaks from the pipes and connections prior to the experiment. While one tactician turned the valve open another timed 15 seconds of flow and the valve was then closed. After
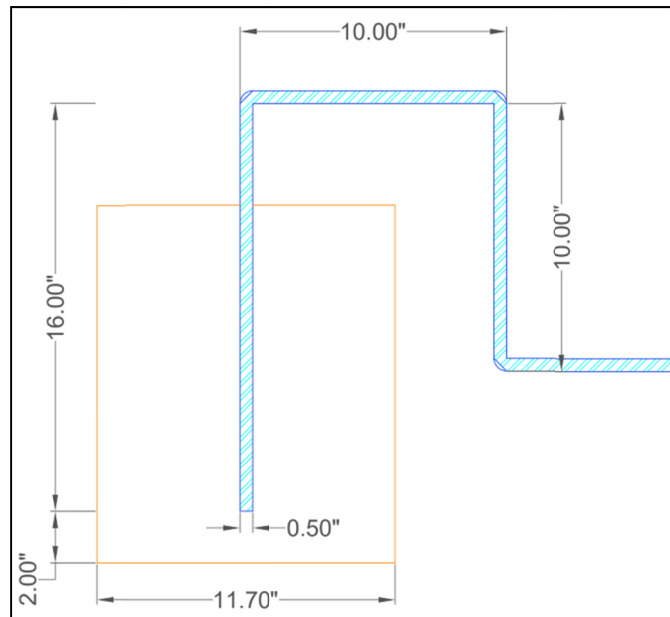
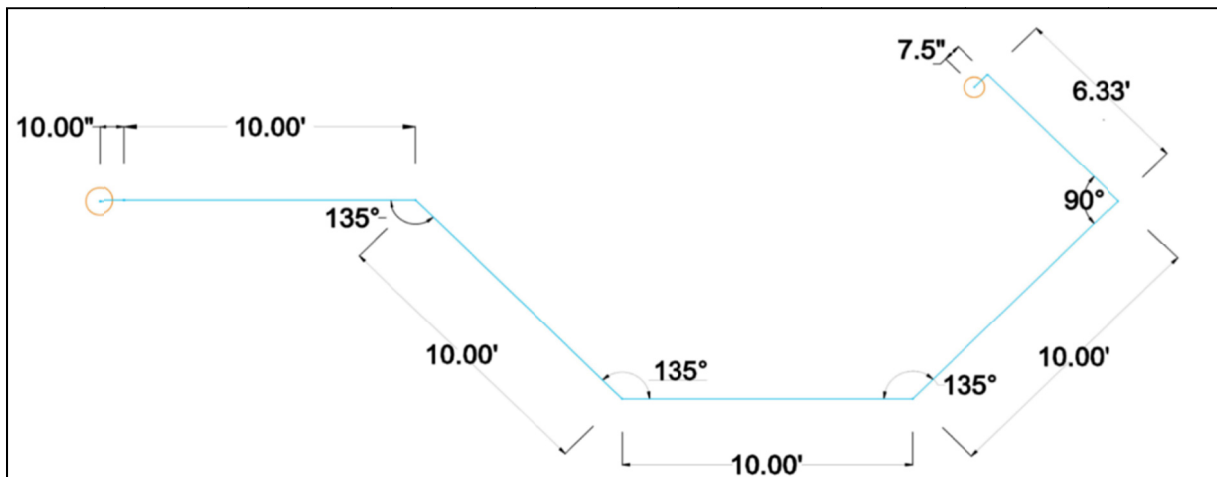**Fig. 1   Elevation view of inlet hydraulic system.**

Fig. 2   Plan view of hydraulic system.

Fig. 3   PVC pipe system used in the research study.

three trials of each of the five different pressures of 1, 1.5, 2, 2.5, and 3 heads of pressure (h_p), the volumetric flow rate was measured by dividing the volume by the time for each trial. The three trial values for each pressure were averaged out to have consistent volumetric flow rate.

To have a basis of comparison, a system was also constructed with a 4" PVC pipe following the same steps listed above, but because of its short length the loss due to friction would become so small that it would become negligible. The velocity was then measured using Eq. (1). With both the experimental and theoretical velocities known various calculations and relationships were made using a combination of the equations listed above.

4. Discussion of Results

The theoretical predictions and test results are discussed in this section. Table 1 and Table 2 show the relationship between the average velocity through the system and the pressure losses that are followed by it. Minor loss is due to the various connections of the pipe and major loss is due to the length of the pipe and the roughness of the material of the pipe. However, both types of losses are functions of velocity as seen in Eq. (3) and Eq. (4) and are exponentially related to one another. One can see in the pressure loss equations that velocity is squared, therefore the faster the flow the

more pressure one can expect to lose to both deviations from a straight path (minor loss) and the friction that the flow experiences from the inside of the pipe containing it (major loss). However, at such low velocities there is still a clear increase in volumetric flow rate Q at the outlet of the system as seen in Table 1. To further conceptualize the amount of pressure loss that the system experienced it is necessary to look at the percentage variations from the tests ran with only a 4" long pipe and compare the differences. Table 2 depicts the difference in volumetric flow rate that the longer pipe which is exposed to more friction has in relation to the very short pipe where friction is negligible. As velocity of the flow increases so does the volumetric flow rates for both systems but the short pipe with no friction increases at a much steeper rate. At $P = 3'$, the system has a 22.8% loss of pressure when compared to a no loss system, and at $P = 1'$ there was only a 11.75% loss due to the friction of the system. This increase in velocity attributes to more loss due to the friction of the surface area of the pipe itself which contacts the water. This can be limited by using a straighter pipe, a larger diameter, less velocity, shorter pipe, and a pipe constructed out of material with a lower friction coefficient. The most important parameter in this is the speed of the fluid since it is the only parameter that is squared in the loss equations. In this experiment the pipe material, length, temperature

Table 1 Velocity vs. pressure losses.

Velocity (ft/s^2)	H_L major (ft)	H_L min (ft)
1.102	0.184	0.0453
1.166	0.206	0.0507
1.237	0.231	0.0570
1.314	0.261	0.0644
1.366	0.283	0.0677

Table 2 Pressure head vs. Q actual vs. % loss.

H_p (ft)	Q_{avg} short pipe (ft^3/s)	Q_{avg} long pipe (ft^3/s)	Pressure loss (%)
1	0.00306	0.00271	11.75
1.5	0.00317	0.00276	13.0
2	0.00326	0.00281	14.4
2.5	0.00346	0.00287	17.0
3	0.00377	0.00291	22.8

and diameter of the pipe were left constant with velocity being the variable by having different pump pressures to isolate one factor for precision.

Figs. 4 and 5 help to visualize how much of an effect the properties of a hydraulic system can have on the output volumetric flow rate. While the total pressure loss due to friction of this hydraulic system is shown in Fig. 6, the goal of a hydraulic system is to transport fluid as efficiently as possible but with the losses in this system show engineering judgment dictates the degree of efficiency that can be obtained.
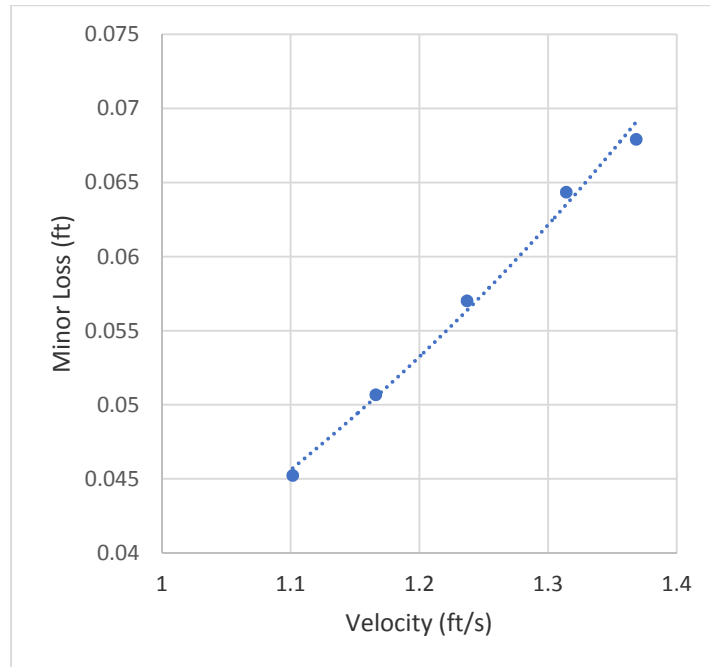
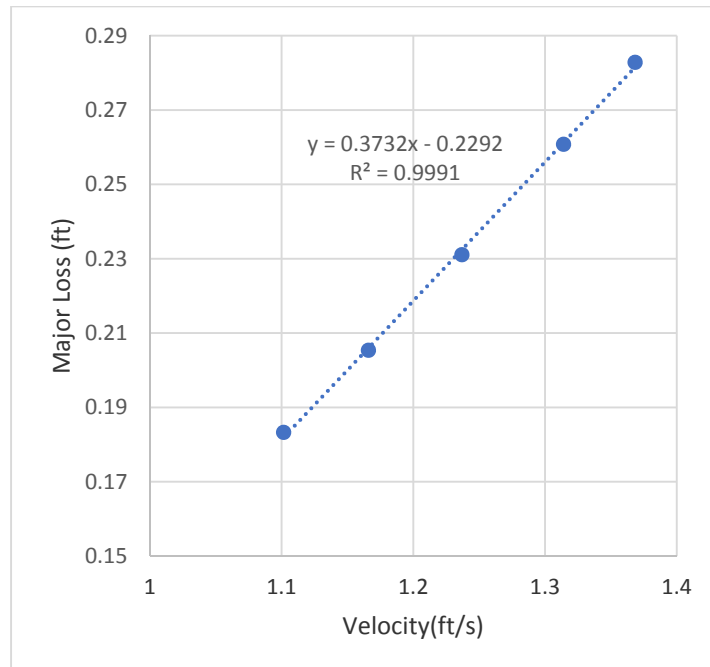**Fig. 4   Minor pressure loss plotted against average velocity.**

Fig. 5   Major pressure loss plotted against average velocity.
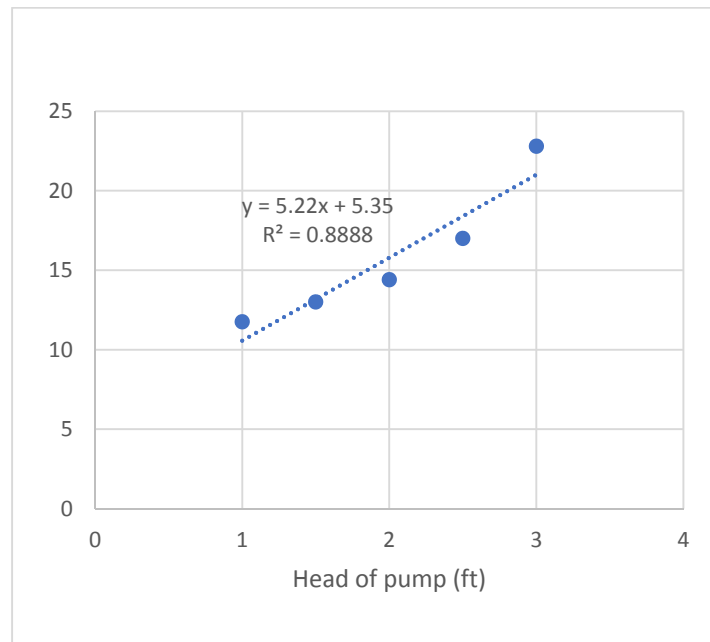
Fig. 6   Total pressure loss due to friction relative to pump pressure.

5. Educational Objectives

The primary objective of this research was to better explore and prove the important relationship between, pipe length, pipe roughness, diameter and specific gravity of the liquid, as well explain and classify the minor and major losses of a hydraulic pipe system. The research team is proud to state that in the matter of personal educational achievements a lot of positive outcomes were reached.

This research assignment also provided a view of communication in the field. Working on this project showed how different cultural and ideological backgrounds can positively affect group ideas. There were several different ways to think which were brought into discussions and helped the group in selecting the best pathways to work. Also, by applying the learnings exposed in class sessions, group meetings and the guidance provided by instructors, the members of the group were able to bring the best performance in this research. The skills learned in this project, will be essential in the future careers of the members.

6. Concluding Remarks

The experiment sheds some light on pipe flow and its parameters when pressure loss was further examined. The team expressed relationships between parameters such as pipe length, pipe roughness, diameter, specific gravity of the liquid, etc. and how each parameter affects the loss in a system. This is important for engineers to understand to be able to make educated design decisions when considering pressure loss. The pressure losses found in this study are magnified when considering larger systems, with lengths of hundreds or thousands of miles. Even the smallest fraction of a percent of pressure loss is important when designing billion-dollar pipe systems. This experiment helps engineers ask important questions such as, how the material of this pipe will affect its volumetric flow rate at the end of the pipe. Or what is the optimum velocity of flow where the minimum loss occurs while still discharging enough fluid. The answers to these questions are not as simple as this experiment but it is a good basis to apply to real life scenarios in the future.

The comprehension of such topics and one's ability to make correct calculations and decisions accordingly are what separates an average person from an engineer. The reason engineers are respected and compensated as much as they are is because of their ability to apply past

knowledge from previous experiments into the field and get appropriate results. To be successful in the field of engineering, the arsenal of a well-rounded engineer should consist of understanding of theories presented in the classroom and capability to apply that knowledge into solving real life problems.

Acknowledgments

The student research team would like to show recognition to Dr. Tadeh Zirakian and Dr. David Boyajian, Professors of Civil Engineering in the Department of Civil Engineering and Construction Management at California State University, Northridge for sharing their knowledge on water recourses and guiding them to successfully complete this research endeavor.

References

[1] Saleta, M. E., Tobia, D., and Gil, S. 2005. "Experimental Study of Bernoulli's Equation with Losses." *American Journal of Physics* 73 (7): 598-602. doi: 10.1119/1.1858486.

[2] Lindeburg, M. R. 2018. *PE Civil Reference Manual*. Kaplan: Professional Publications, Inc.

[3] Çengel, Y. A., and Cimbala, J. M. 2018. *Fluid Mechanics: Fundamentals and Applications*. New York: McGraw-Hill.

[4] Duveen, D. I., and Klickstein, H. S. 1954. "Medallic Portraiture of Antoine Laurent Lavoisier." *Journal of Chemical Education* 31 (6): 308-9.

[5] Lindsay, G. A. 1952. "Pressure Energy and Bernoulli's Principle." *American Journal of Physics* 20 (2): 86-88. doi:10.1119/1.1933123.

[6] Wisniak, J. 2011. "Conservation of Energy Readings on the Origins of the First Law of Thermodynamics. Part II." *Educacion Quimica* 19 (3): 216. doi: 10.22201/fq.18708404e.2008.3.258.

Appendix

The following is a sample calculation to find the effective pressure loss in the system when the head of the pump was set to 3 feet. By applying the givens and lugging into the volumetric flow rate equation the team was able to find the velocity in the system. Finding the velocity is the key to the calculating the Reynolds number and the major and minor pressure losses in this hydraulic system.

$$P_1 = 3ft$$

$$Q_1 = 0.00588 \, ft^3/s$$

$$\rho = 1.94 \, slugs/ft^3$$

$$D = .0416 \, ft$$

$$\mu = 2.34 \, lbf * s/ft^2$$

$$g = 32.2 \, ft/s^2$$

$$L = 50.567 \, ft$$

$$Q = \rho V A \quad \rightarrow V = \frac{Q_1}{\rho A} = \frac{.00588}{1.94 \times (.00136)} = 2.23 \, ft/s$$

$$Re = \frac{\rho V D}{\mu} = \frac{1.94 \times (2.23) \times (.0416)}{2.34 \times 10^{-5}} = 7691.02$$

$$f = 0.008 \quad b/c \quad \in \approx 0$$

$$h_{L\,min} = \sum K_L \frac{V^2}{2g}$$

$$h_{L\,min} = 2.4 \times \frac{(2.23)^2}{64.4} = 0.185$$

$$h_{L\,major} = f \times \frac{L}{D} \times \frac{V^2}{2g}$$

$$h_{L\,major} = 0.008 \times (\frac{50.567}{0.0416}) \times (\frac{2.23^2}{64.4}) = 0.7509$$

$$h_L = h_{L\,min} + h_{L\,major}$$

$$h_L = 0.185 + 0.7509$$

$$h_L = 0.9359$$